



eBook:
Organoid
analysis

SARTORIUS



eBook: Organoid analysis

Contents

Introduction

Interview: Improving organoid analysis with new developmental approaches

Application Note: Real-time live-cell analysis of 3D organoid growth in Matrigel[®] domes

Report: A fast and simple fluorometric method to detect cell death in 3D intestinal organoids

Application Note: Label-free, real-time live cell assays for 3D organoids embedded in Matrigel[®]

Review: Intestinal organoids: a model to study the role of microbiota in the colonic tumor microenvironment



Introduction

The use of organoids as *in vitro* models is on the rise. These models can effectively imitate *in vivo* pathophysiology, making them a valuable tool for studying human development and disease. However, to optimize their use in different research areas, variability needs to be reduced, and technology pipelines must be developed to accurately image, monitor and quantify these complex 3D cell models.

Many current techniques used for characterizing and visualizing organoids are low throughput and not scalable for screening, involving time-consuming, expensive and manual processes for acquisition of organoid images. Furthermore, current methods often require third-party software for endpoint analysis or the addition of fluorescent markers, which provide limited quantitative information and can also perturb biological responses.

In this eBook, we will explore various methods for characterizing and analyzing organoids, including a culture platform for tumour organoids with a novel geometrical format to facilitate high-throughput screening, a fluorometric method to detect cell death in organoids, and label-free, real-time live-cell analysis of 3D organoids in Matrigel. We'll also look at how organoids can be applied to study the role of the microbiota in the colonic tumor microenvironment.



Annie Coulson
Digital Editor,
BioTechniques
a.coulson@future-science-group.com

Improving organoid analysis with new developmental approaches

Having gained experience developing patient-derived organoids during her postdoc training and quickly identifying them as an hot prospect for the life sciences, Alice Soragni (right) founded her lab at the University of California, Los Angeles (UCLA; CA, USA) with a mission statement focused to develop sophisticated organoid models for cancer research. Now her lab includes a basic research line focused on protein aggregation in cancer, which runs alongside her investigations of tumor organoid models for rare cancers.



Here, we discuss her work on the development of tumor organoid models for benign conditions and rare malignant cancers, how she has altered her platform to improve screening and analysis and the exciting insights being derived from single-organoid analysis approaches.

Can you tell us about the organoid development side of your lab and the rare cancers that you're trying to mimic?

We focus on rare cancers because although these cancers are rare individually, about one in four cancers diagnosed are considered a rare cancer. Due to their rarity, there are frequent challenges with these cancers as most have not been studied as thoroughly as more common types, leading to a paucity of information. Often, we don't know what's driving the tumors, we don't understand their biology or physiology and we don't have therapies that work. For us, this highlights a lot of unmet needs in the rare cancer space. One of the most basic needs is to develop models that we can use to investigate the biology of these cancers and to use in precision medicine.

To address this, we have developed a fairly unique platform. Since the very beginning, we were interested in taking advantage of the tractable aspect of organoids and finding ways to screen them broadly with as many perturbations as you can think of. The original hurdle to overcome here is that it's technically challenging to screen things in three dimensions. We developed a platform that allows us to screen in three dimensions with a really simple workaround: changing the geometry with which we seeded our tumor organoids, growing them in mini-rings of Matrigel lining the periphery of each well.

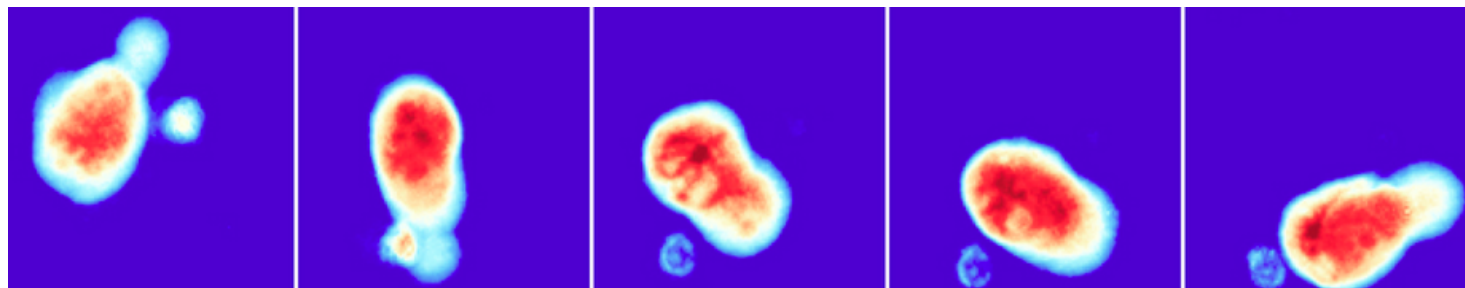
Through our platform, we can grow tumor organoids for any type of cancer you can think of, perform high-throughput screening and obtain results within a week of tissue procurement, surgery or biopsy.

What was the geometric change you made to your organoids and how has this improved screening capabilities?

To achieve high-throughput screening, you need an easy way to use robotics, liquid handlers and automation. A lot of the instruments involved in these processes are targeted to the center of plate wells and typically organoids are grown in a Matrigel domes or layers at the center of the wells.

To adapt to this requirement of high-throughput screening, we wanted to ensure that the center of the well is empty so that you can use any type of automation without worrying about touching your organoids or aspirating them away. We developed a method that generates organoids in ring-like structures around the edge of the well. It's a very simple change, but that's all it takes. We can generate these rings the same day of surgery, and then we never have to touch the cells again. The cells will grow, and we do everything with automation, giving you a very robust setup for your screening.

Improving organoid analysis with new developmental approaches



Organoids developed in the Soragni Lab. Credit: Alice Soragni.

What cell sources do you derive your organoids from?

For the vast majority of our work, we work with clinical samples obtained directly from the operating room, or any type of procedure that is removing a tumor or cancerous tissue from a patient. We can also use tissue that we obtained from biopsies. We also do a lot of platform development work, to optimize and improve this platform. For that kind of optimization work, we still use cell lines but grown in 3D.

What are the advantages of using these patient-derived or clinical samples over immortalized cell lines?

Cell lines have provided a wealth of knowledge to our research community that shouldn't be underestimated. However, there is a lot of brilliant work out there showing that just passaging your cells or keeping them long-term in culture leads to changes in their biology. These immortalized cell lines have been growing for decades and so are often no longer similar to the tumor they originated from. Clinical samples, however, are as close as you can get to an individual's disease. This means that you can derive greater, and likely more applicable, insights into the biology of a tumor from organoids derived from these samples. They also bear much greater weight in precision medicine when testing treatment options for a specific patient. That's why we are trying to keep it as close as possible to the patient and why we prioritize short-term culture over expanding cells for our screenings.

What recent developments have enabled you to generate patient-derived organoids?

A few years ago, anytime I would present our work I would have someone come up to me and say, "We were trying this 40 years ago and it always failed, so it's not going to work, right?" But now we have much better ways to collect cells and isolate them in a gentle manner, we have better matrixes to grow them in, more consistency and media conditions that have been optimized over decades by many labs. We have really good methods to keep the cells happy and grow them in conditions that are physiological, so it is really the combination of all of these advances that has enabled the type of work we do so that we can establish these cultures. With the process of generating organoids so dramatically improved, the next step is the analysis of these cultures, for which methods that are also rapidly improving.

What are some currently evolving areas of organoid development that excite you?

A lot of the existing platforms have focused on doing population-level readouts, including our own. In these studies, you take your organoids, add the drug of choice and then measure the response at a well level. With multiple organoid cultures in each well, this means you don't pick up on the heterogeneous responses that may occur within each well.

I think some of the most exciting platforms coming out now are looking at responses at the single-

Improving organoid analysis with new developmental approaches

organoid level. We have recently published a paper in Nature Communications that details our efforts to do this. What's exciting about our technical development is that it gives us a method of analyzing single-organoid responses in a label-free, noninvasive manner, and in real-time.

Our technology requires no manipulation to change or label the organoids, we can just literally look at what's happening over time. We're using this method called high-speed live-cell interferometry in collaboration with the laboratory of Mike Teitell here at UCLA. This is a technique to measure the weight of cells, so to measure the weight of the organoids, and see how that changes over time as we add different drugs. I think these forms of analysis are really powerful and they're being further enhanced by machine learning-type approaches to sort organoids and analyze data.

Are there any exciting discoveries that have been made using a single-organoid approach to analysis?

It's the little unexpected things. For example, the paper I mentioned we have coming out is focused on developing the platform. We were using these run of the mill, been around forever, predictable HER2-positive and HER2-negative breast cancer cell lines. They should have responded very differently to agents that target HER2 and we did see that. In general, the cell line with highly overexpressed HER2 responded very well to these drugs while the one that doesn't have high expression responded much less.

But when analyzed at the individual organoid level, we picked up small subpopulations in the highly overexpressed HER2 lines that actually did not respond to therapy. They hung in there. I think that's so interesting. You have these very well-established cell lines that you think will be entirely homogeneous, right? But instead, even there we can pick up very

small subpopulations of organoids that behave differently.

I think the ability to identify single organoids with differential responses, as we now apply these techniques to clinical samples, is going to be crucial because it's going to allow us to see if there are any cell populations that will be resistant to otherwise successful treatment options. It may even allow us to determine ahead of time whether, even after an initial response in the patient, resistance may develop later on. This allows us to study what makes these organoids different coupling our approach with next-generation sequencing, and how we could potentially target the resistant populations, possibly with a different agent. It's one of the things we're very excited about.

If there was one thing you could ask for to improve your investigations with patient-derived organoids, what would it be?

I would love to get access to even more rare tumors, to model them and study their biology. I also think the ability to do spatial investigations and to capture real-time responses is game-changing, there are so many promising technologies being developed and published, including very exciting machine learning-based approaches to data analysis. The field is in such a good place right now. To have ways to apply all these new developments and analyses to understand rare and ultrarare tumors is what I hope we will continue to do.

Keywords or phrases:

Organoid, Organoid QC, cancer cells, Stem Cells, 3D *in vitro* model, Organoid Live-Cell Imaging, Organoid culture, Label-free Organoid, Organoid formation & maturation, differentiation, Organoid maintenance, expansion in Matrigel domes

Real-time Live-Cell Analysis of 3D Organoid growth in Matrigel® domes

Introduction

Recent advances in organoid technology have opened up new horizons for translational human disease research, disease modeling, regenerative medicine and predictive precision therapies¹.

Organoids are differentiated primary micro tissues formed from a variety of stem cells (SCs) that can be established within 3D extracellular matrices to mimic *in-vivo* architecture and genetic diversity¹. As self-organizing and self-renewing structures, organoids have a distinct advantage over traditional monolayer culture techniques and hold unprecedented potential for various applications^{1,2}. In order to effectively use these models in basic research, disease modeling and drug screening, specific and reliable *in-vitro* culture and analysis methods are required.

Currently, characterization and optimization of organoid cultures are limited in their ability to objectively monitor these 3D structures as they form and grow over time. The Incucyte® Organoid Analysis Software Module provides a solution to standardize and automate organoid culture workflows, simplifying culture characterization and optimization.

Assay Principle

This application note describes the use of the Incucyte® Live-Cell Analysis System and Incucyte® Organoid Analysis Software Module to study the formation and growth of organoid cultures. A proprietary Brightfield (BF) image acquisition approach enables real-time kinetic imaging of 3D organoids embedded within Matrigel® domes. Organoid size, count and morphology measurements are automatically

plotted over time to provide insight on organoid differentiation and maturation characteristics.

Here we describe validation methods and data demonstrating the ability to kinetically visualize and quantify organoid formation and growth in Matrigel® domes.

Find out more: www.sartorius.com/en/applications/life-science-research/cell-analysis/live-cell-assays/cell-monitoring-workflows/organoid-culture-qc

Material & Methods

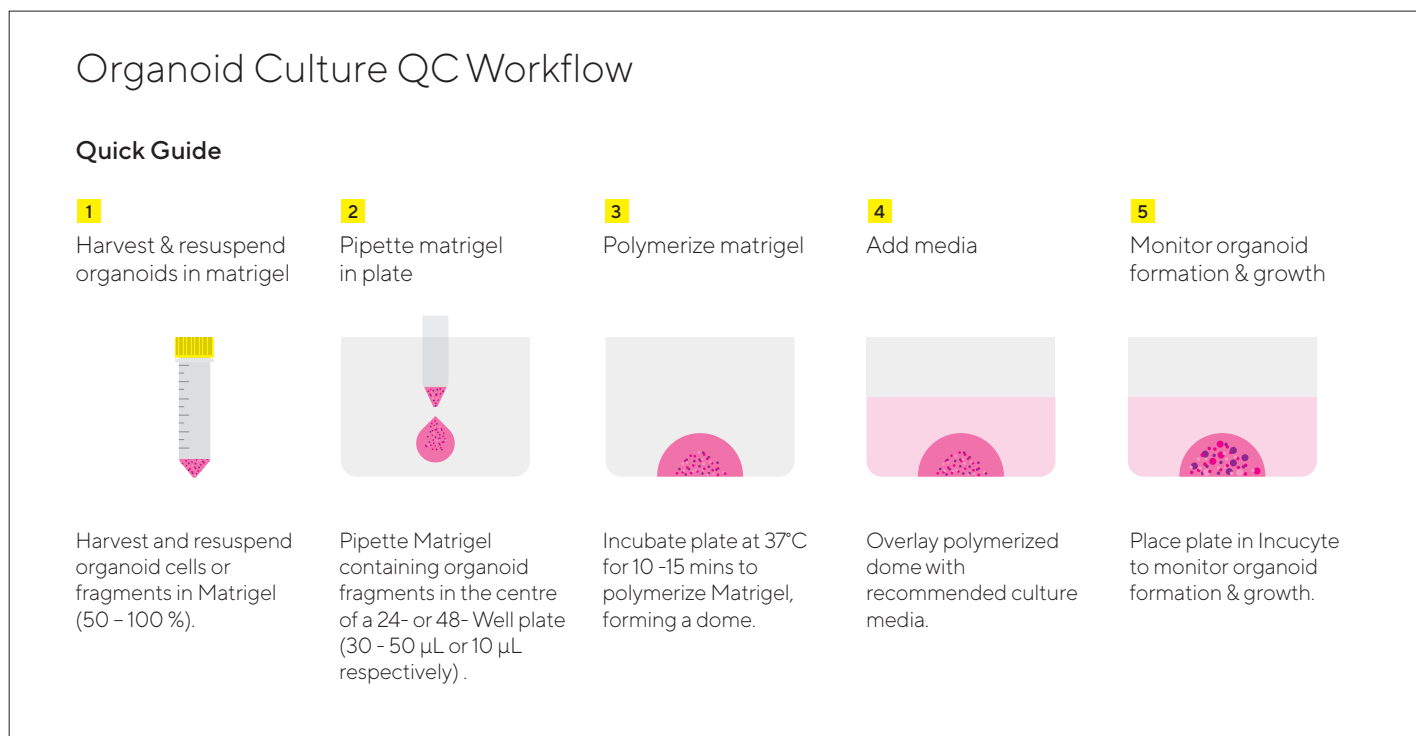


Figure 1. Assay Workflow

1. Organoids of interest are harvested according to model-specific guidelines and organoid pellet is re-suspended in Matrigel® (50 - 100%)
2. Matrigel® containing single cells or organoid fragments is pipetted into the center of a well in a 24-well or 48-well tissue culture treated plate to form a dome (10 µL in 48-well plate, 30 µL- 50 µL in 24-well plate).
3. Plate is placed in a humidified incubator to polymerize Matrigel® (37° C, 10 - 15 minutes).

4. Cell type-specific growth media is added on top of solidified dome (250 µL/well in 48-well plate or 750 µL/well in 24-well plate).
5. Organoid formation and growth is monitored in an Incucyte® (Organoid scan type, 4X, 6 hour repeat scanning, 5 - 10 days). Organoid size (maturation) is reported in real-time based on brightfield image analysis.

Organoid culture reagents were obtained from StemCell Technologies unless otherwise noted. Mouse Intestinal (#70931), Pancreatic (#70933) and Hepatic (#70932) organoids were embedded in Matrigel® domes (Corning #356231) in 24-well or 48-well flat bottom TC-treated microplates (Corning #3526, 3548 respectively) and cultured in organoid growth medium (IntestiCult™ OGM Cat. #06005; PancreaCult™ OGM #06040; HepatiCult™ OGM #06030) supplemented with 100 units/100 µg per mL Pen/Strep (Life technologies). Organoid formation and growth was monitored in an Incucyte® at 6 hour intervals for up to 10 days.

Monitoring and quantifying organoid growth in Matrigel® domes.

Mouse intestinal, pancreatic and hepatic organoids were embedded in Matrigel® domes (50% or 100%) in 24-well plates and imaged every 6 hours.

Organoid growth, differentiation and maturation was measured using Incucyte's automated Organoid Software Analysis Module which tracks changes in organoid size (area) over time.

Figure 2 illustrates the software's ability to visualize as a single in focus 2D image, individual organoids embedded throughout the Matrigel® dome (top). Zoomed in BF images (bottom) and time-courses revealed cell type-specific morphological features and growth profiles respectively. Note the comparable rapid growth (time-courses) and size (BF images) of mature hepatic and pancreatic organoids in contrast to intestinal organoids, which appear smaller and exhibit a distinct budding phenotype as they mature.

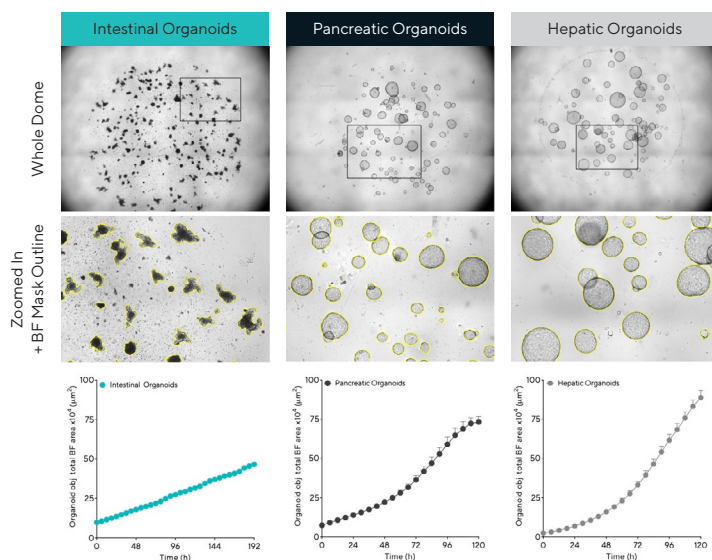


Figure 2. Acquisition and quantification of organoid growth in Matrigel® domes. Mouse intestinal (1:3 split, 50% Matrigel), pancreatic (1:5 split, 100% Matrigel®) and hepatic organoids (1:40 split, 100% Matrigel®) were embedded in Matrigel® domes in 24-well plates and imaged every 6 h in an Incucyte. Brightfield (BF) images of the entire Matrigel® dome (top) show organoid maturation 6 days post seeding. Note accurate segmentation (yellow outline mask) and distinct phenotypes of mature organoids (bottom). Time-course plots showing the individual well total BF area (μm^2) over time (h) demonstrate cell type specific organoid growth. All images captured at 4X magnification. Each data point represents mean \pm SEM, n = 4 wells.

Optimization and characterization of organoid cultures using real-time kinetic measurements.

Defining optimal culture conditions and regimes are critical for establishing healthy cultures for use in downstream studies. Objectively defining parameters such as seeding densities, passage frequency and ensuring cultures have differentiated and display appropriate morphology is key.

Measuring proliferation to optimize growth conditions and seeding densities

To optimize organoid seeding density, mouse hepatic organoids were embedded in Matrigel® domes (100%) in 48-well plates at multiple split ratios (1:10–1:40 split). BF images and quantification of organoid area demonstrated

that organoid growth rate and size is proportional to the number of cells seeded (Figure 3). Organoids seeded at the highest density appeared larger ($>500 \mu\text{m}$ diameter) and exhibited rapid growth reaching maximal size ($73.4 \times 10^4 \mu\text{m}^2 \pm 2.3$ mean \pm SEM, n = 14 wells) within 120 h (Figure 3, BF images and total area time-course respectively). Conversely, at lower densities while the organoid maturation phase was extended ($28.6 \times 10^4 \mu\text{m}^2 \pm 2.9$ mean \pm SEM, n = 14 wells at 120 h, total area), the greatest growth potential (size) was observed (Figure 3, average area time-course).

Measuring morphological features to define optimal organoid maturation phase

To define optimal organoid passaging frequency, mouse hepatic organoids were embedded in Matrigel® domes (100%) and imaged in an Incucyte® for 8 days. Hepatic organoids are typically ready for passaging when

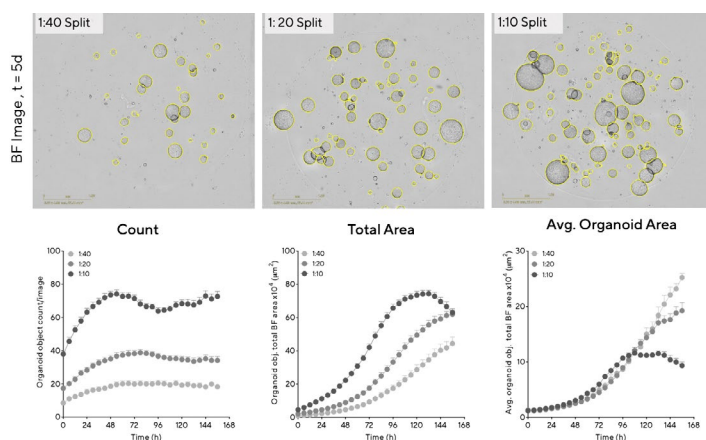
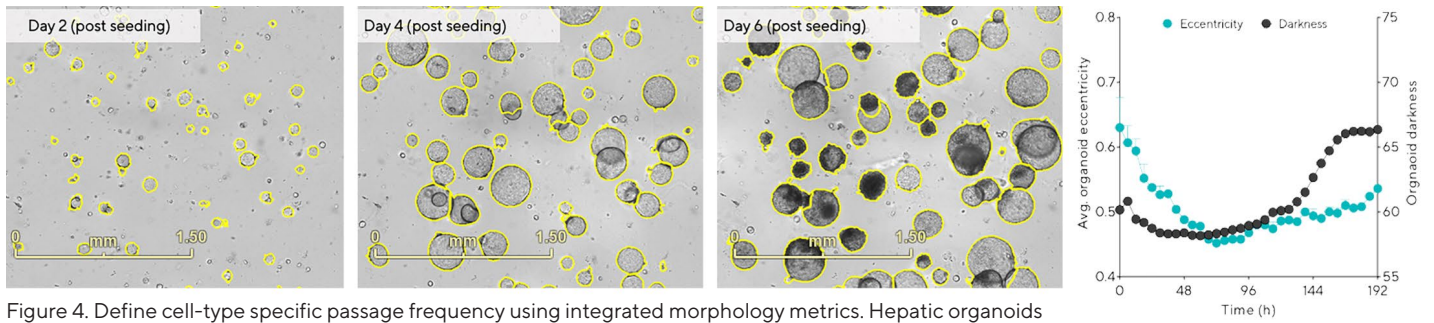


Figure 3. Determine optimal conditions for maximal organoid expansion. Mouse hepatic organoids were embedded in Matrigel® domes (100%) in 48-well plates at multiple seeding densities. BF Images (5 d post seeding) and time-courses of individual well area and count demonstrate density-dependent organoid growth. Data were collected over 168 h at 6 h intervals. All images captured at 4X magnification. Each data point represents mean \pm SEM, n=14 wells.

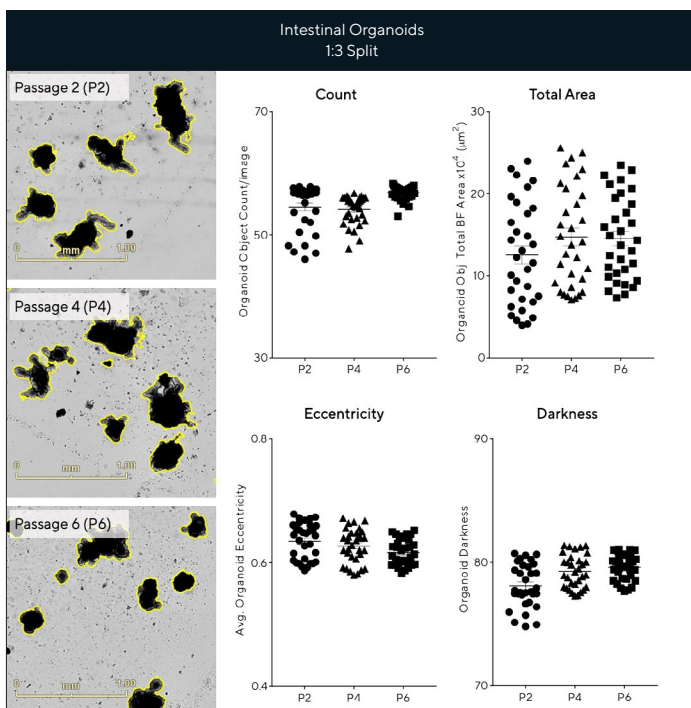


the majority of organoids have reached their maximum growth and have not collapsed³. Representative BF Images (Figure 4) show that 2 days post seeding, cultures are not yet ready for passaging as the majority of organoids are less than 100 μ m in diameter and exhibit clear lumens. A decline in eccentricity was also observed within 48 h as organoids formed and became more rounded (Figure 4, time-course). The optimal period for passaging this culture occurred between days 4 and 5, when most organoids within the dome had reached maximal size, exhibited a rounded morphology and had not collapsed (Figure 4). The time-course shows a marked increase in organoid darkness as collapsed organoids darkened over time (Figure 4, time-course, >96 h).

Tracking organoid differentiation and growth efficiency through passages

Under routine culture conditions, organoid morphology and growth capabilities are expected to remain consistent across multiple passages.

To assess intestinal organoid expansion and growth efficiency across passages a number of parameters were kinetically quantified (Figure 5). When maintained at a consistent density, intestinal organoids exhibited comparable count, area, eccentricity and darkness measurements across passages (Figure 5). Representative BF images (7 d) also demonstrate maintenance of distinct budding phenotype across multiple passages. Figure 5 exemplifies the amenability of this imaging and analysis approach to support robust and reproducible assessment of long-term organoid expansion.



Conclusions

In this application note, we demonstrate the use of the Incucyte® Live-Cell Analysis system, in combination with the Incucyte® Organoid Analysis Software Module, to facilitate kinetic assessment of organoid formation and growth. We have demonstrated:

- The ability to automatically locate and analyze 3D organoids embedded within Matrigel® domes in both 24-and 48-well plates.
- The use of integrated, real-time label-free metrics to optimize and define culture conditions and regimes.
- Optimal periods for passaging or extension of organoid cultures based on integrated morphological parameters.
- Use of this approach to assess culture quality during extended passaging.

References

- 1 D. e. al., "Disease modeling in stem cell-derived 3D organoid systems," *Cell Press*, vol. 23, no. 5, pp. 393-410, 2017.
- 2 G. e. al., "Long-term expansion, genomic stability and in vivo safety of adult human pancreas organoids.," *BMC Dev Biol*, vol. 4, 2020.
- 3 "StemCell Technologies," [Online]. Available: <https://www.stemcell.com/mouse-hepatic-progenitor-organoid-culture-supplementary-protocols.html>.



The Gold Standard in RUO Growth Factors & Cytokines

Ensure reproducibility and scalability when characterizing your cells with Sartorius' broad range of high-quality research use only (RUO) growth factors and cytokines. These products are manufactured to the highest quality standards in a dedicated, animal-free facility and distributed according to a Quality Management System that is certified for compliance with ISO 9001. Leveraging recombinant DNA technology, they do not contain any animal-derived components or contaminants so you can have peace of mind.

Simplifying Progress



Learn More

SARTORIUS

A fast and simple fluorometric method to detect cell death in 3D intestinal organoids

Konstantin J Bode^{1,4}, Stefanie Mueller¹, Matthias Schweinlin², Marco Metzger³ & Thomas Brunner^{*1}

ABSTRACT

Organoids recapitulate the (patho)physiological processes in certain tissues and organs closer than classical cell lines. Therefore, organoid technology offers great potentials in drug development and testing, and personalized medicine. In particular, organoids can be used to study and predict drug-induced toxicity in certain tissues. However, until today few methods had been reported to analyze cell death in 3D-microtissues in a quantitative manner. Here, we describe a novel fluorometric method for the quantitative measurement of specific organoid cell death. Organoids are stained simultaneously with the cell impermeable nuclear dye propidium iodide and cell permeable Hoechst33342. While Hoechst allows in-well normalization to cell numbers, propidium iodide detects relative proportion of dead cells independent of hydrogel. Measurement and analysis time, as well as usability are drastically improved in comparison to other established methods. Parallel multiplexing of our method with established assays measuring mitochondrial activity further enhances its applicability in personalized medicine and drug discovery.

METHOD SUMMARY

We developed a fluorometric method to quantify cell death in intestinal organoids based on DNA staining for normalization and cell permeability for cell death. The method, independent of cell number over a wide range, can be used to study toxic effects of drugs on intestinal organoids or other 3D microtissues, and can be combined with photometric assessment of mitochondrial respiration.

KEYWORDS:

cell death • DNA dyes • fluorescence • intestine • organoids • personalized medicine

¹Department of Biology, University of Konstanz, Konstanz, Germany; ²Department of Tissue Engineering & Regenerative Medicine (TERM), University Hospital Würzburg, Würzburg, Germany; ³Translational Centre Regenerative Medicine TLC-RT, Fraunhofer Institute for Silicate Research (ISC), Würzburg, Germany; ⁴Co-operative research training school 'Advanced in vitro test systems for the analysis of cell-chemical interactions in drug discovery & environmental safety (InViTe)', University of Konstanz, Konstanz, Germany; *Author for correspondence: thomas.brunner@uni-konstanz.de

BioTechniques 67: 00-00 (July 2019) 10.2144/btn-2019-0023

Organoids grown from tissue-specific stem cells have become useful tools to study physiological and pathophysiological processes in an *in vitro* system much closer to the *in vivo* situation than cell lines. In 2009, Sato *et al.* described a method on how isolated primary intestinal crypt cells can be cultured over prolonged periods of time [1]. Today, organoids are being generated from nearly every tissue and any organism [2–4]. They are defined as organ-like structures, which self-organize in 3D. Comprised of several tissue- and organ-specific cell types, including stem cells, organoids are capable of fulfilling a variety of organ-specific functions, for example, excretion or secretion [5].

Intestinal organoids are being used to study not only basic intestinal physiology [6], but also pathophysiological processes, for example, TNF α -induced epithelial cell death during inflammatory bowel disease [7,8]. Moreover, intestinal organoids have been used to study host–pathogen interactions, for example, during Zika virus infection [9]. Importantly, intestinal organoids may also represent an unlimited source of transplantable tissue suitable for regenerative medicine. In a proof-of-principle study murine intestinal organoids were successfully transplanted into the severely damaged colon of mice suffering from inflammatory bowel disease. Organoids not only engrafted functionally into the colon but regenerated the damaged epithelium [10]. Tumor tissue-derived organoids also provide interesting tools to study tumor-specific drug responses as well as tumor diversity *ex vivo*, for example, in colorectal tumors [11,12]. Therefore, primary and tumor organoids are being and will be frequently employed for drug discovery [13] and toxicity testing, but also drug screening in patient-derived malignant tissue [14–16]. In this regard, patient-derived tumor organoid (PDOs) from pancreatic, prostate and gastrointestinal cancer are being used to model drug responses of patient-specific tumors in comparison to normal parental tissue [17–22]. This is of particular interest, as in gastrointestinal cancer it has been demonstrated that the parental and the PDO mutational spectra overlap up to 96%, on top of histological similarities [21].

Thus, by closely resembling the primary tumor *in vivo* drug testing in PDOs represents a further step towards personalized medicine [21]. Moreover, organoid-like 3D primary cell culture models are being effectively used to screen a large number of emerging oncology compounds for their cytostatic and cell death-promoting activity [23].

A significant problem of cell death screening in organoids is their 3D culture in extracellular matrix, which allows visual qualitative assessment of cell death, but impedes quantitative analysis of cell death. We have previously described the use of a modified MTT staining method to detect organoid survival, specifically, cell death in culture [24]. However, this method is strongly affected by mitochondrial respiration and only an indirect measure of cell survival, specifically, cell death. Other studies have used staining of dying organoids with propidium iodide (PI) and Hoechst33342 (Hoechst) to quantify cell death, employing complex and thus time-consuming high-content imaging [25].

The aim of this study was therefore to develop a simple, practical and quantitative method to study cell death in organoids using PI and Hoechst. While Hoechst is being used to normalize cellularity, PI uptake serves as a measure of cell death. The normalization allows sensitive cell death detection

over a wide range of cell densities. Fluorescence in 3D cultures can be quantified using a conventional plate reader. The increase of the PI signal relative to the constant Hoechst signal allows calculation of chemotherapeutic drug treatment-specific organoid cell death. Moreover, this method can be multiplexed with our previously described organoid-optimized MTT assay, allowing simultaneous analysis of respiration/survival and cell death. Thus, in comparison to other known assays our method offers a fast and simple protocol to detect organoid cell death in cell culture plates with minimal computational power and reduced overall costs.

MATERIALS & METHODS

Mice

C57BL/6 wild-type mice were bred and kept in individually ventilated cages at the central animal facility of the University of Konstanz.

Generation of intestinal organoids

Intestinal crypts were isolated as described previously with minor changes [1,24]. In brief, the small intestine of 8–16-week old C57BL/6 wild type mice was cut open longitudinally. Villi were removed by scraping with a microscope slide. Then, the intestine was cut into 3–4 cm pieces, washed three times with cold Ca^{2+} - and Mg^{2+} -free PBS, and incubated with 2 mM EDTA in PBS for 30 min at 4°C on a rotating wheel. All subsequent steps until seeding were performed on ice. Supernatant was removed and the tissue was filled up with fresh PBS. After shaking to remove residual villi, fresh PBS was replaced. This step was repeated and each fraction was checked for crypt/villus ratio under the microscope. Up to four crypt-containing fractions were pooled, filtered through a 70- μm cell strainer, centrifuged at $100 \times g$ (3 min, 4°C) and resuspended in 5 ml PBS for crypt counting under the microscope. Numbers of crypts required for further culture were centrifuged at $80 \times g$ (3 min, 4°C) and the pellet was resuspended in Matrigel (BD Biosciences) or in Basement Membrane Extract (BME) (Type II, R&D). A total of 200–300 crypts were seeded per well in 8 μl Matrigel or BME into a 96-well flat-bottom transparent cell culture plate (Sarstedt). Seeded crypts were incubated for 20 min at 37°C to let Matrigel and BME solidify. Then, 80 μl of complete crypt

culture medium per well was added dropwise (Advanced DMEM/F12, 0.1% BSA, 2 mM L-glutamine, 10 mM HEPES, 100 U/ml penicillin, 100 $\mu\text{g}/\text{ml}$ streptomycin, 1 mM N-acetyl cysteine (Sigma), 1 \times B27 supplement, 1 \times N2 supplement (Gibco), 50 ng/ml mEGF, and 100 ng/ml mNoggin (Peprotech). hR-spondin-1 was added as conditioned medium of hR-spondin-1-transfected HEK 293T cells to a final volume of 25% (v/v) crypt culture medium. Organoids were cultured at 37°C in a 5% CO_2 atmosphere for 3 days before cell death induction.

Generation of tumoroids

Organoids from tumors (tumoroids) were generated as described previously with slight modifications [26]. Briefly, the small intestine of $\text{APC}^{\text{Min/+}}$ mice was opened longitudinally. Tumors were isolated from intestinal tissue with scissors and forceps and cut into small pieces. Subsequently, tumor fragments were washed three times with ice cold Ca^{2+} - and Mg^{2+} -free PBS, and incubated in digestion buffer (DMEM, 2.5% FBS, 100 U/ml penicillin, 100 $\mu\text{g}/\text{ml}$ streptomycin, 200 U/ml Collagenase IV, 125 $\mu\text{g}/\text{ml}$ Dispase II) for 1 h at 37°C, 5% CO_2 . Tissue suspensions were shaken every 15 min. After 1 h tumor fragments were allowed to settle for 1 min. Subsequently, the supernatant was harvested and centrifuged at $200 \times g$ for 3 min at room temperature. The pellet was resuspended in 5 ml PBS and filtered through a 70 μm and a 40 μm cell strainer. After centrifugation ($200 \times g$ for 3 min) cells were resuspended in 500 μl PBS and counted. Cell numbers were adjusted to 1.5×10^4 cells/50 μl Matrigel/BME. Complete growth medium with only 50 ng/ml mEGF was added. The culture medium was changed every 4 days. Tumoroids were split according to their density, but in general every week. Thus, medium was removed and tumoroids were incubated in cold PBS for 1 h on ice. Subsequently, Matrigel/BME was dissociated mechanically with a pipet tip and tumoroids were resuspended in cold PBS. Then, tumoroids were centrifuged at $200 \times g$ for 3 mins and the pellet was resuspended in TrypLE Express (Thermo Fisher) for 15 min at RT. Tumoroid fragments were then centrifuged at $350 \times g$ for 3 min and split in a 1:4 ratio for further culture.

Culture of human intestinal organoids

Human intestinal organoids were generated and cultured as described previously [27]. Frozen organoids were thawed and cultured in a mixture of 50% basal medium containing 500 ng/ml hR-spondin-1, 50 ng/ml mEGF, 100 ng/ml mNoggin, 10 nM [Leu15]-Gastrin I, 10 mM Nicotinamide, 500 nM A83-01 (TGF β inhibitor), 10 μM SB202190 (p38/MAPK inhibitor), 10 μM Y-27632 (ROCK inhibitor) and 50% Wnt3A-conditioned medium. Growth medium was replenished every second to third day, and organoids were passaged weekly.

Staining of organoids with PI & Hoechst

Intestinal organoids in Matrigel/BME were stained with PI and Hoechst at a final concentration of 10 $\mu\text{g}/\text{ml}$ each. Staining solution (dyes in PBS) was directly added to culturing medium after treatment. Organoids were stained for 30 min at 37°C, 5% CO_2 for subsequent analysis on the plate reader or by fluorescence microscopy. Then, staining medium was removed and replenished with fresh phenol-red free medium before analysis.

Fluorometric quantification of specific cell death in intestinal organoids

Cell death was induced in organoids and cell lines as indicated. Before measurement, staining medium was replaced with fresh phenol-red free medium. Stained organoids still embedded in hydrogel (Matrigel/BME) were measured in a plate reader (Tecan M200 Pro). Measurements were taken from the top. First, the gain was set to the wells for the highest expected cell death (PI) and the lowest expected cell death (Hoechst). Then, Z-position was determined automatically from the corresponding wells and was checked for values between 1.5×10^6 and 1.6×10^6 μm . Subsequently, fluorescence was measured with 25 flashes, with an integration time of 20 μs . Lag and settle time were set to 0 s. For each well, 4×4 measurements were taken with a border of 1 mm added around the measurement points. Excitation and emission wavelengths for PI were 535 nm and 617 nm, respectively, and for Hoechst 361 and 486 nm, respectively. During the measurement, all wells were first measured for PI fluorescence and after a 30-s delay for Hoechst fluorescence.

Calculation of PI/Hoechst ratio & treatment-specific organoid cell death

The PI/Hoechst ratio was calculated by dividing PI by Hoechst RFUs:

$$\frac{PI}{H} \text{ ratio} = \frac{RFU (PI)}{RFU (Hoechst)}$$

Using PI/Hoechst ratio, treatment specific organoid cell death was calculated:

$$\text{treatment-specific organoid cell death [\%]} = \left(\frac{x(\text{sample})}{z(\text{STS})} \right) \times 100 - y(\text{ut})$$

Each sample was divided by the mean of all staurosporine (STS)-treated organoids and resulting values multiplied by 100. Then, mean of all untreated (ut) organoids was subtracted to set ut organoids to 0.

Determination of organoid viability & specific organoid death using MTT reduction

Organoid viability was assessed by 3-(4,5-dimethylthiazol-2-yl)-2,5-diphenyltetrazolium bromide (MTT) reduction as described in [24]. Briefly, after cell death induction MTT solution was added to the organoid culture to a final concentration of 500 µg/ml and incubated for 1 h at 37°C, 5% CO₂. Then, medium was discarded and 20 µl of 2% SDS solution in H₂O was added to solubilize the hydrogel (Matrigel/BME) for 1 h at 37°C. Subsequently, 80 µl of DMSO was added and incubated for 1 h at 37°C to solubilize the reduced MTT. The optical density was then measured at 562 nm in a plate reader (Tecan M200 Pro).

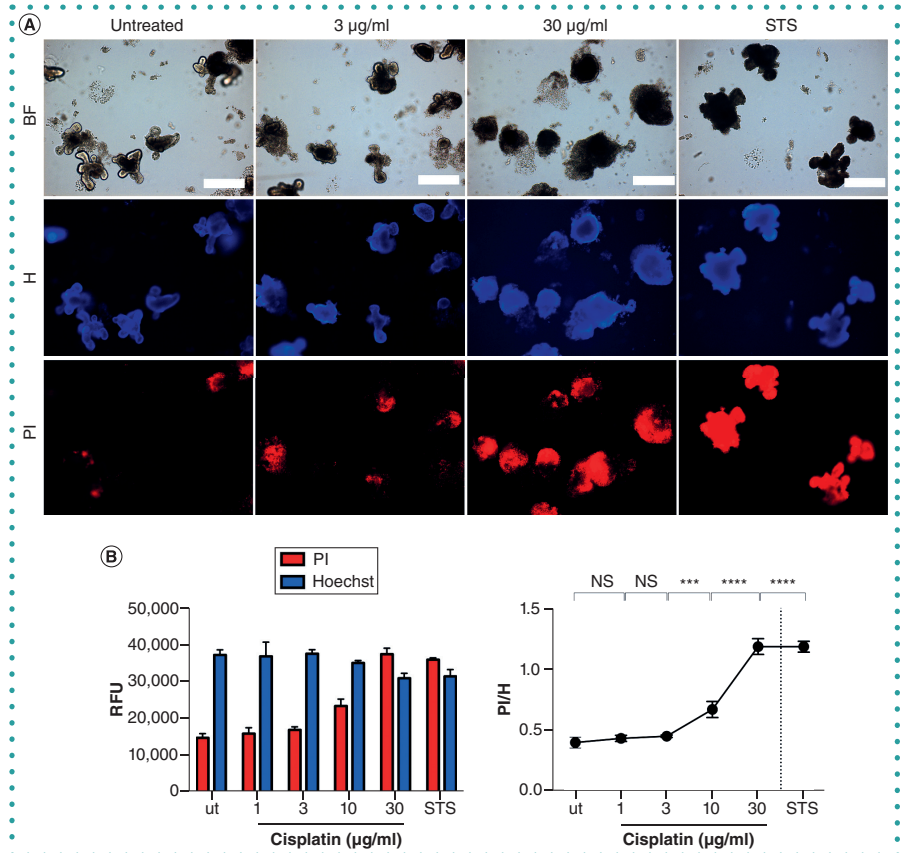


Figure 1. Quantification of PI and Hoechst in 3D organoids. Organoids were treated with indicated concentrations of cisplatin overnight. Then, organoids were stained with PI and Hoechst, and fluorescence was detected. (A) Representative BF and fluorescence microscopic images of untreated, 3 µg/ml cisplatin, 30 µg/ml cisplatin, and STS (5 µM) treated organoids (scale bar = 200 µm). (B) Left side: RFUs of PI and Hoechst over all concentrations. Right side: ratio of PI/H over the whole dose response. Mean ± standard deviation; n = 3 with technical triplicates. ***p ≤ 0.001; ****p < 0.0001.

BF: Brightfield; H: Hoechst; NS: Nonsignificant; PI: Propidium iodide; RFU: Relative fluorescence unit; STS: Staurosporine.

Quantification of intracellular ATP

Intracellular ATP was quantified with the CellTiter-Glo® 3D cell viability assay according to manufacturer's protocol

(Promega). Briefly, after treatment medium was removed and cells were lysed in 100 µl pre-warmed CellTiter-Glo 3D reagent. Then, samples were incubated for 30 min on an

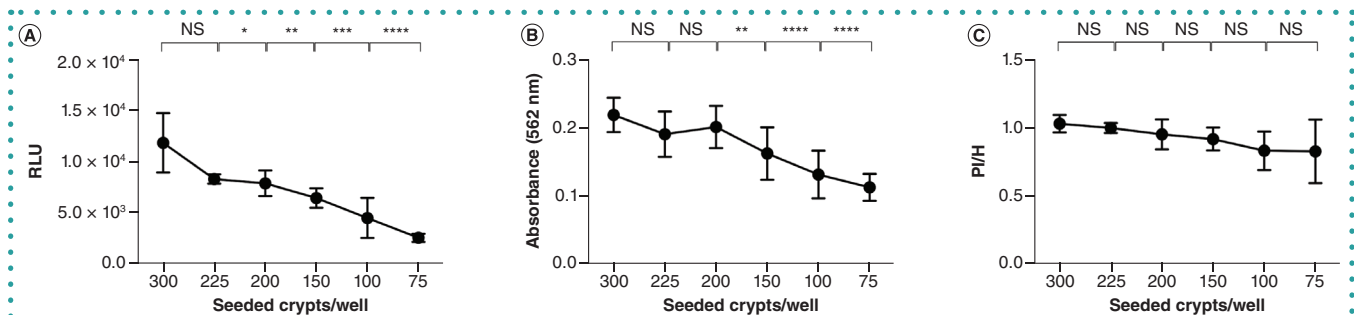


Figure 2. Assay comparison with different organoids densities. Murine intestinal crypts were seeded in indicated concentrations and grown for 3 days into organoids. Then, organoids were analyzed using CellTiterGlo (A) or MTT reduction assay (B). For PI/H fluorescence quantification (C), organoids were treated with 10 µg/ml cisplatin overnight before measurement.

*p ≤ 0.05; **p ≤ 0.01; ***p ≤ 0.001; ****p < 0.0001.

NS: Nonsignificant; PI/H: Propidium iodide and Hoechst; RLU: Relative luminescence unit.

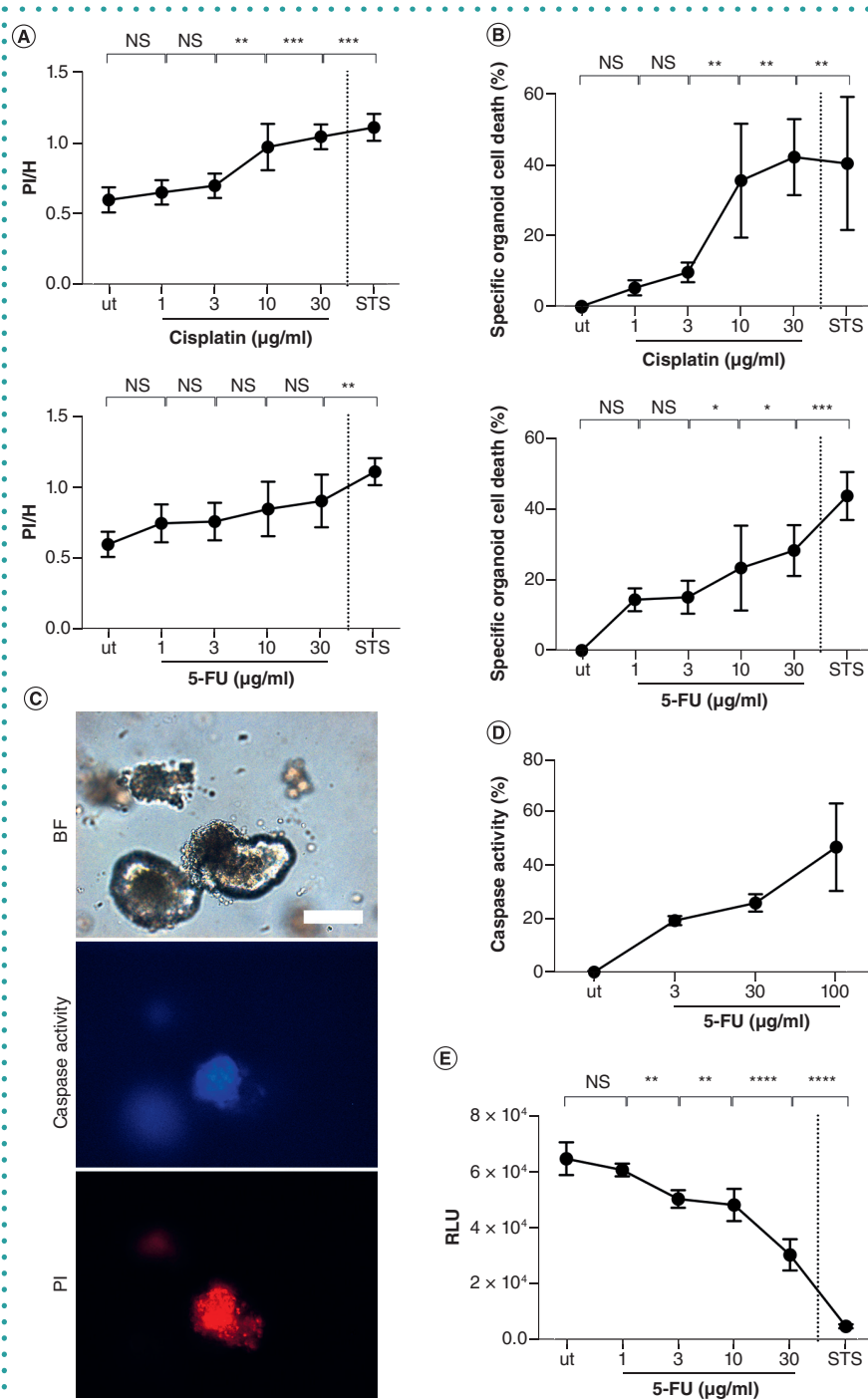


Figure 3. Propidium iodide and Hoechst quantification to calculate specific organoid cell death. Organoids were treated with indicated concentrations of chemotherapeutics and STS (5 µM) overnight. Then, PI/H ratio and treatment-specific organoid cell death were calculated (A & B). (C) Fluorescence image of organoid treated with 10 µg/ml cisplatin overnight and then stained with PI and Caspase 3/7 substrate. (D) Caspase activity was calculated with signal of Caspase 3/7 substrate. (E) RLU, illustrating intracellular ATP-content, assessed with CellTiterGlo (scale bar = 85 µm). Mean ± standard deviation; n = 3 with technical triplicates.

*p ≤ 0.05; **p ≤ 0.01; ***p ≤ 0.001; ****p < 0.0001.

5-FU: 5-fluorouracil; BF: Brightfield; H: Hoechst; PI: Propidium iodide; RLU: Relative luminescence unit; STS: Staurosporine.

orbital shaker and luminescence was recorded afterwards using a plate reader (Tecan M200 Pro).

Analysis of activated effector caspases

Activation of effector caspases 3 and 7 was performed with CellMeter™ Live Cell Caspase 3/7 Assay Kit (blue fluorescence) according to manufacturer's protocol (AAT Bioquest). In brief, organoids were stained with ApoBrite™ U470 Caspase 3/7 substrate for 2 h at 37°C before treatment. Then, cell death was induced and organoids stained additionally with PI. Subsequently, fluorescence was recorded microscopically (Zeiss Axio Observer.Z1), and quantitatively at 380 nm (ApoBrite) and 617 nm (PI) using a plate reader (Tecan M200 Pro).

Fluorescence microscopy

Intestinal organoids were stained with nuclear dyes as described above and subsequently analyzed in hydrogel (Matrigel/BME) on a Zeiss Axio Observer.Z1 microscope. Brightfield images were taken with Palm-ROBO and fluorescence pictures with AxioVision Software (Zeiss).

Statistical analysis

Statistical analysis was performed using GraphPad Prism (GraphPad Prism Software, Inc.). Unless denoted otherwise, experiments were repeated three times with technical triplicates. One-way ANOVA with Dunnett's multiple comparisons test was performed.

RESULTS & DISCUSSION

Cell death analysis in intestinal organoids in general, and its detection by PI/Hoechst staining in particular, requires precise experimental timing. If organoids are grown for prolonged periods of time dead cells accumulate in the lumen leading to a strong PI background. Therefore, all experiments shown were performed at day 3 after crypt isolation, whereas thawed human organoids were analyzed at day 3 after splitting. Moreover, cell death induction was performed overnight to ensure proper cell membrane disintegration and nuclear staining, independent of the mode of cell death. Initially, organoids were stained for various amounts of time (5–60 min) to assess the optimal duration of staining with both dyes. As stainings with both dyes were

close to completion at 30 min, this time point was used for all subsequent experiments (Supplementary Figure 1).

Figure 1A shows exemplified pictures of murine intestinal organoids treated with the chemotherapeutic drug cisplatin or the pan-kinase inhibitor STS as a positive control. Whereas the PI signal gradually increased with increasing cisplatin concentrations, the Hoechst signal was only slightly attenuated (Figure 1A & B). Quantification of PI and Hoechst fluorescence enabled ratio formation, thus normalizing dying/dead organoids (PI-positive) to total DNA (Hoechst-positive). This ratio is significantly different between untreated organoids and increasing cisplatin concentrations, or STS (Figure 1C). The internal normalization by Hoechst staining stabilized measurements over a wide range of organoid densities (Figure 2B, right), whereas other established methods assessing cellular respiratory potential revealed a strong dependency on cell numbers (Figure 2A & B).

Having established that the ratio of PI/Hoechst signal gradually increased with increasing cell death induced by increasing cisplatin concentrations (Figure 1B), we next aimed at assessing treatment-specific organoid cell death in response to the chemotherapeutic drugs cisplatin and 5-fluorouracil (5-FU) (Figure 3A & B). Increasing concentrations of either chemotherapeutic drug resulted in an increased PI/Hoechst ratio, and an increase in the calculated treatment-specific organoid cell death (Figure 3A & B). To assess whether cell death observed was associated with apoptosis, caspase activity was analyzed in parallel with PI staining, demonstrating double-positive cells (Figure 3C) and a dose-dependent increase in caspase activity (Figure 3D). Currently, organoid cell death is frequently assessed indirectly by a reduction in intracellular ATP levels [28,29]. The direct comparison revealed that PI/Hoechst staining detects chemotherapy-induced organoid cell death as sensitively as intracellular ATP levels (Figure 3B & E).

In order to verify that cell death analysis by PI/Hoechst staining is not limited to murine primary intestinal organoids, we also assessed cell death quantification with PI/Hoechst staining in murine tumoroids (Figure 4A–C) and human intestinal organoids (Figure 4D), confirming the

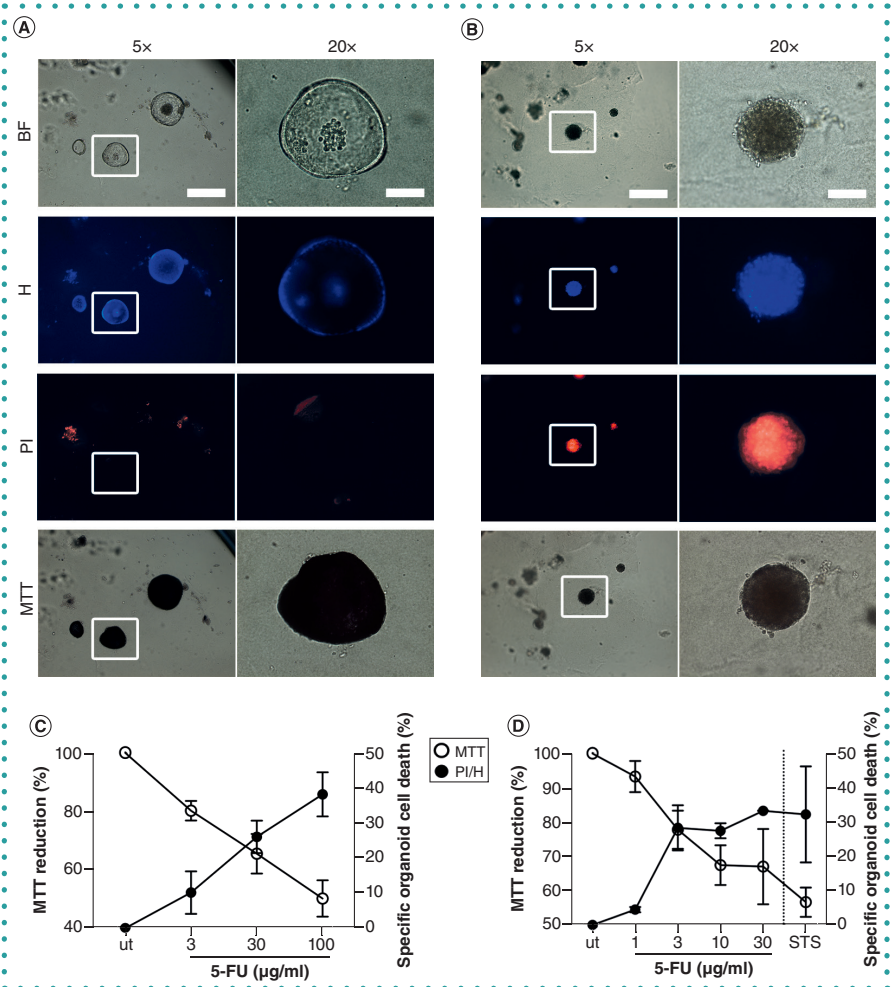


Figure 4. Multiplexing PI/H quantification with MTT-reduction assay. Tumoroids from APC^{+/+} mice were treated with indicated concentrations of 5-FU overnight, stained with PI/H, and fluorescence was quantified. Subsequently, MTT solution was added and MTT reduction was measured. BF and fluorescence microscopic images of untreated tumoroid (A) and 5-FU treated tumoroid (B). (C) PI/H fluorescence derived specific organoid cell death (right axis), MTT reduction (left axis). (D) Human organoids treated with cisplatin. PI/H ratio and MTT reduction were measured, and specific organoid cell death as well as MTT reduction were calculated thereof. Scale bar (5×) = 350 μm, (20×) = 85 μm. Mean ± standard deviation; n = 3 with technical triplicates. 5-FU: 5-fluorouracil; BF: Brightfield; PI/H: Propidium iodide and Hoechst.

suitability of this method for other types of organoids.

We next set to multiplex cell death assessment by combining PI/Hoechst staining with our previously established method of measuring organoid viability by MTT reduction [30]. Therefore, organoids from intestinal tumors of APC^{min} mice (tumoroids) were treated with indicated concentrations of 5-FU, stained with PI and Hoechst, and fluorescence was measured. Subsequently, PI/Hoechst-stained tumoroids were further incubated with MTT and reduction capacity was analyzed by absorbance of the resulting formazan at 562 nm. Whereas viable (ut)

tumoroids efficiently reduced MTT to purple formazan (Figure 4A), tumoroids treated with 5-FU showed morphological disintegration and failed to reduce MTT (Figure 4B). A decrease in MTT reduction was paralleled by an increase in PI signal, but stable Hoechst staining (Figure 4A & B). Quantification of PI/Hoechst fluorescence and formazan absorption enabled calculation of treatment-specific organoid cell death (PI/Hoechst), which inversely correlated with decreased MTT reduction (Figure 4C). Multiplexing PI/Hoechst staining and MTT reduction was also confirmed by analyzing cisplatin-induced cell death in human intestinal organoids (Figure 4D). These data ►

demonstrate that analysis of cell death by PI/Hoechst and cell survival by MTT reduction can be combined in 3D organoid cultures.

In conclusion, we here present a fast and simple method to quantify organoid cell death by measuring PI and Hoechst fluorescence in 3D in a plate reader. The method is cheap, reliable, and does not require commercially available kits, or complicated and time-consuming high content imaging analysis [21,25]. Thus, it is applicable for analysis of treatment-specific organoid death without the need to invest in expensive equipment or bioinformatics. By multiplexing this method with assays assessing respiratory changes, such as MTT reduction [30], information gain is increased and might help to distinguish between direct cell death-inducing agents and inhibitors of cellular respiration and metabolism.

FUTURE PERSPECTIVE

Organoid technology is already being used to investigate patient-specific drug response. Usage of patient-derived organoids is likely to increase in the future. Thus, fast and robust methods are needed to quantitatively assess cell death in organoids. As our method is fast and simple it can be used frequently in the future to quickly assess death-inducing effects of drugs in PDOs.

SUPPLEMENTARY DATA

To view the supplementary data that accompany this paper please visit the journal website at: www.future-science.com/doi/suppl/10.2144/btn-2019-0023

ACKNOWLEDGMENTS

APC^{Min/+} mice were a kind gift of Jan Paul Medema, Amsterdam, The Netherlands.

AUTHOR CONTRIBUTIONS

KJB designed the study, conducted most experiments, and wrote the manuscript, SM conducted some experiments and contributed to the manuscript, MS and MM gave technical advice, refined the manuscript and provided human jejunal cells, TB designed and supervised the study, provided funding and finalized the manuscript.

AUTHOR CONTRIBUTIONS

APC^{Min/+} mice were a kind gift from Jan Paul Medema, Amsterdam, The Netherlands.

FINANCIAL & COMPETING INTERESTS DISCLOSURE

KJ Bode was supported by a fellowship from the Baden-Württemberg Ministry of Science, Research and Art-funded Co-operative research training school 'Advanced *in vitro* test systems for the analysis of cell-chemical interactions in drug discovery and environmental safety' (InViTe). The authors have no other relevant affiliations or financial involvement with any organization or entity with a financial interest in or financial conflict with the subject matter or materials discussed in the manuscript apart from those disclosed.

No writing assistance was utilized in the production of this manuscript.

ETHICAL CONDUCT OF RESEARCH

The authors state that they have obtained appropriate institutional review board approval or have followed the principles outlined in the Declaration of Helsinki for all human or animal experimental investigations. In addition, for investigations involving human subjects, informed consent has been obtained from the participants involved.

OPEN ACCESS

This work is licensed under the Attribution-NonCommercial-NoDerivatives 4.0 Unported License. To view a copy of this license, visit <http://creativecommons.org/licenses/by-nc-nd/4.0/>

REFERENCES

Papers of special note have been highlighted as: • of interest

- Sato T, Vries RG, Snippert HJ *et al.* Single Lgr5 stem cells build crypt-villus structures *in vitro* without a mesenchymal niche. *Nature* 459(7244), 262–265 (2009).
- Murine intestinal organoids are described for the first time.
- Marx V. Tissue engineering: organs from the lab. *Nature* 522(7556), 373–377 (2015).
- Clevers H. Modeling development and disease with organoids. *Cell* 165(7), 1586–1597 (2016).
- Meneses AMC, Schmeberger K, Kruitwagen HS *et al.* Intestinal organoids – current and future applications. *Vet. Sci.* 3(4), (2016).
- Lancaster MA, Knoblich JA. Organogenesis in a dish: modeling development and disease using organoid technologies. *Science* 345(6194), 1247125 (2014).
- Yu H, Hasan NM, In JG *et al.* The contributions of human mini-intestines to the study of intestinal physiology and pathophysiology. *Annu. Rev. Physiol.* 79, 291–312 (2017).
- Howell KJ, Krawczyk J, Nayak KM *et al.* DNA methylation and transcription patterns in intestinal epithelial cells from pediatric patients with inflammatory bowel diseases differentiate disease subtypes and associate with outcome. *Gastroenterology* 154(3), 585–598 (2017).
- Grabinger T, Bode KJ, Demgenski J *et al.* Inhibitor of apoptosis protein-1 regulates tumor necrosis factor-mediated destruction of intestinal epithelial cells. *Gastroenterology* 152(4), 867–879 (2017).
- Murine and human intestinal organoids are used to investigate the interplay of TNF and cIAP1 in the intestine.

- In JG, Foulke-Abel J, Estes MK, Zachos NC, Kovbasnjuk O, Donowitz M. Human mini-guts: new insights into intestinal physiology and host-pathogen interactions. *Nat. Rev. Gastroenterol. Hepatol.* 13(11), 633 (2016).
- Yui S, Nakamura T, Sato T *et al.* Functional engraftment of colon epithelium expanded *in vitro* from a single adult Lgr5(+) stem cell. *Nat. Med.* 18(4), 618–623 (2012).
- Lee SH, Hu W, Matulay JT *et al.* Tumor evolution and drug response in patient-derived organoid models of bladder cancer. *Cell* 173(2), 515–528 e517 (2018).
- Roerink SF, Sasaki N, Lee-Six H *et al.* Intra-tumour diversification in colorectal cancer at the single-cell level. *Nature* 556(7702), 457–462 (2018).
- Ranga A, Gjorevski N, Lutolf MP. Drug discovery through stem cell-based organoid models. *Adv. Drug Deliv. Rev.* 69–70, 19–28 (2014).
- Astakhina A, Grainger DW. Critical analysis of 3-D organoid *in vitro* cell culture models for high-throughput drug candidate toxicity assessments. *Adv. Drug Deliv. Rev.* 69–70, 1–18 (2014).
- Bulin AL, Broekgaarden M, Hasan T. Comprehensive high-throughput image analysis for therapeutic efficacy of architecturally complex heterotypic organoids. *Sci. Rep.* 7(1), 16645 (2017).
- Kondo J, Ekawa T, Endo H *et al.* High-throughput screening in colorectal cancer tissue-originated spheroids. *Cancer Sci.* 110(1), 345 (2018).
- Gao D, Vela I, Sboner A *et al.* Organoid cultures derived from patients with advanced prostate cancer. *Cell* 159(1), 176–187 (2014).
- Huang L, Holtzinger A, Jagan I *et al.* Ductal pancreatic cancer modeling and drug screening using human pluripotent stem cell- and patient-derived tumor organoids. *Nat. Med.* 21(11), 1364–1371 (2015).
- Hubert CG, Rivera M, Spangler LC *et al.* A three-dimensional organoid culture system derived from human glioblastomas recapitulates the hypoxic gradients and cancer stem cell heterogeneity of tumors found *in vivo*. *Cancer Res.* 76(8), 2465–2477 (2016).
- Perkhofer L, Frappart PO, Muller M, Kleger A. Importance of organoids for personalized medicine. *Per. Med.* 15(6), 461–465 (2018).
- Vlachogiannis G, Hedayat S, Vatsiou A *et al.* Patient-derived organoids model treatment response of metastatic gastrointestinal cancers. *Science* 359(6378), 920–926 (2018).
- Patient-derived organoids are used as preclinical models.
- Wills ES, Drenth JP. Building pancreatic organoids to aid drug development. *Gut* 66(3), 393–394 (2017).
- Saeed K, Rahkama V, Eldfors S *et al.* Comprehensive drug testing of patient-derived conditionally reprogrammed cells from castration-resistant prostate cancer. *Eur. Urol.* 71(3), 319–327 (2017).
- Grabinger T, Luks L, Kostadinova F *et al.* *Ex vivo* culture of intestinal crypt organoids as a model system for assessing cell death induction in intestinal epithelial cells and enteropathy. *Cell Death Dis.* 5, e1228 (2014).
- Jabs J, Zickgraf FM, Park J *et al.* Screening drug effects in patient-derived cancer cells links organoid responses to genome alterations. *Mol. Syst. Biol.* 13(11), 955 (2017).
- The authors use the nuclear dyes Hoechst and propidium iodide to microscopically assess organoid cell death.
- Xue X, Shah YM. *In vitro* organoid culture of primary mouse colon tumors. *J. Vis. Exp.* 75, e50210 (2013).
- Schweinlin M, Wilhelm S, Schwedhelm I *et al.* Development of an advanced primary human *in vitro* model of the small intestine. *Tissue Engineering Part C: Methods.* 22(9), 873–883 (2016).
- Boehnke K, Iversen PW, Schumacher D *et al.* Assay establishment and validation of a high-throughput screening platform for three-dimensional patient-derived colon cancer organoid cultures. *J. Biomol. Screen.* 21(9), 931–941 (2016).
- Francies HE, Barthorpe A, McLaren-Douglas A, Barendt WJ, Garnett MJ. Drug sensitivity assays of human cancer organoid cultures. *Methods Mol. Biol.* 1–12 (2016).
- Organoids are employed for a drug sensitivity assay using a commercial kit detecting changes in intracellular ATP.
- Grabinger T, Delgado E, Brunner T. Analysis of cell death induction in intestinal organoids *in vitro*. *Methods Mol. Biol.* 1419, 83–93 (2016).
- The authors describe how MTT reduction in intestinal organoids can be used to assess cell death.

Keywords or phrases:

Organoids, Organoid Assay, Organoid Analysis Software, Organoid Growth, Organoids Embedded in Matrigel

Label-Free, Real-Time Live Cell Assays for 3D Organoids Embedded in Matrigel®

Miniver Oliver¹, Tim Jackson¹, Sandra Leibel², Kalpana Barnes¹, Tim Dale¹

1. Essen BioScience, Royston, Hertfordshire, UK

2. Rady Children's Hospital, University of California, San Diego

Introduction

Advances in preclinical *in-vitro* models are crucial for both basic research and drug development across a range of applications. Organoid technologies are increasingly being used as *in-vitro* models of human development and disease as they exhibit structural, morphogenetic and functional properties that recapitulate *in-vivo* pathophysiology.¹ To successfully use these models across a variety of research disciplines and applications, approaches that reduce variability and technology pipelines to image and quantify these complex cell models are required.

Currently, techniques to robustly characterize and visualize these models may be limited by one or more of the following:

- Time-consuming, expensive or laborious acquisition processes.
- Use of third party analysis software.
- Random, end point assessments or indirect (e.g. ATP)

readouts that may overlook key morphological changes over time.

- Requirement to label cells (fluorescence-based quantification), which may be challenging and not amenable to a range of cell types.

The Incucyte® Organoid Analysis Software Module provides a solution to standardize and automate organoid acquisition and analysis workflows, simplifying characterization of these complex cultures.

Assay Principle

This application note describes the use of the Incucyte® Live-Cell Analysis System along with the Incucyte® Organoid Analysis Software Module to study the growth or death of organoids, label-free. A proprietary brightfield image acquisition approach enables real-time kinetic imaging of 3D organoids embedded within a matrix (Matrigel®). Organoid size, count and morphology

measurements are automatically plotted over time to gain in-depth organoid characterization following perturbation. Here we describe validation methods and data demonstrating the ability to kinetically image and quantify the growth, death and morphology of organoids embedded in Matrigel®.

Materials and Methods

Quick Guide

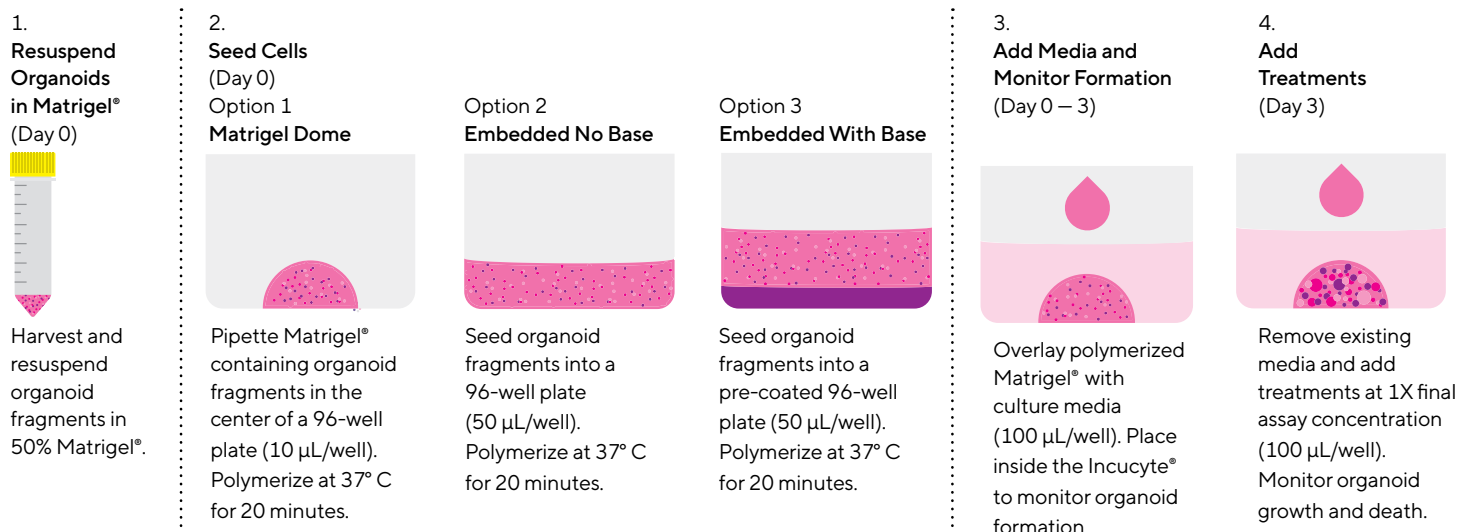


Figure 1: Incucyte® Organoid Assay Workflow

- Organoids of interest are harvested according to model-specific guidelines and resuspended in 50% Matrigel®.
- Matrigel® containing organoid fragments is pipetted into each well of a 96-well tissue culture treated plate utilizing any of following assay formats:
 - **Matrigel® Dome** (Pre-warmed plate; 10 µL/well)
 - **Embedded No Base** (Pre-chilled plate; 50 µL/well)
 - **Embedded With Base** (Pre-coated plate; 50 µL/well)
- Plate is placed in a humidified incubator to polymerize Matrigel® (37° C, 20 minutes).
- Cell type-specific growth media is added on top of polymerized Matrigel® (100 µL/well).
- Organoid formation is monitored in an Incucyte® (Organoid Assay scan type, 4x, 6-hour repeat scanning, 0 – 3 d).
- Post formation, treatments are added (100 µL at 1x final assay concentration (FAC) per well).
- Organoid growth and death is monitored within an Incucyte® every 6 hours for up to 10 days. Organoid metrics (e.g. size, count, eccentricity) are reported in real-time based on brightfield image analysis.

Organoid culture reagents were obtained from StemCell Technologies unless otherwise noted. Mouse intestinal (#70931), hepatic (#70932), human brain (healthy or patient derived; prepared externally) and human lung organoids (cultured by University of California San Diego²) were embedded in Matrigel® (Corning #356231 or #354277 brain organoids) in 96-well flat bottom TC-treated microplates (Corning #3595).

Organoids were cultured in cell type-specific organoid growth medium (e.g. IntestiCult™ OGM Cat. #06005; #06040; HepatiCult™ OGM #06030; STEMdiff™ Cerebral Organoid Kit Cat. #08570) supplemented with 100 units/100 µg per mL Pen/Strep (Life technologies). Organoid formation, growth and death was monitored in an Incucyte® at 6-hour intervals for up to 10 days.

Visualizing and Quantifying Differential Organoid Phenotypes in a 96-Well Assay Format

To evaluate the ability of the Incucyte® Organoid Analysis Software Module to accurately track organoid growth in 96-well plates, mouse intestinal, hepatic, or human whole lung organoids² were embedded in Matrigel® (50 %) and bright-field (BF) images were acquired every 6 hours (Figure 2A).

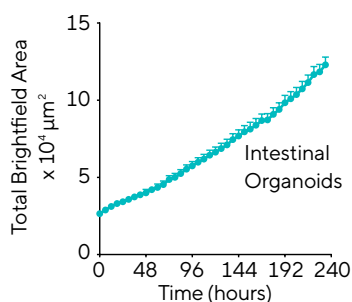
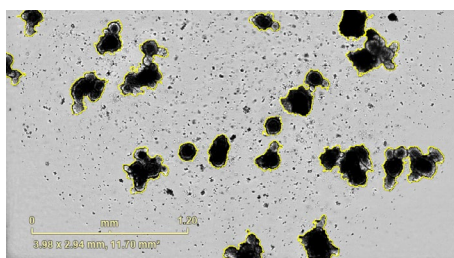
Organoids were automatically located and changes in size (area) were kinetically tracked using Incucyte's Organoid Software Analysis Module. BF area segmentation shown in yellow (Figure 2) enabled label-free quantification of organoid growth and illustrates the software's ability to accurately segment individual objects embedded in Matrigel® across a range of cell types.

Acquired BF images (6 d post seeding) and time-courses (Figure 2A) revealed cell type-specific morphological features and temporal growth profiles respectively. Individual lung organoids appeared larger (400 μm – 1 mm diameter) than

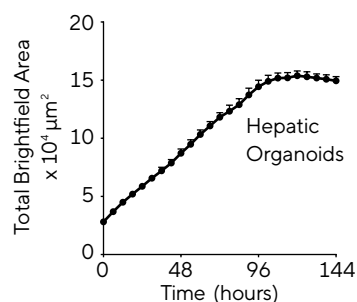
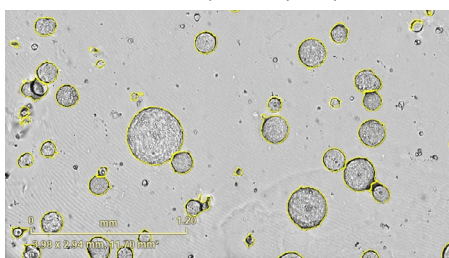
Intestinal (100 - 400 μm) or hepatic (50 - 500 μm) organoids and reached maximal size rapidly (90 h, $22.1 \times 10^4 \mu\text{m}^2 \pm 2.5$ mean \pm SEM, $n = 3$ wells).

To further demonstrate the software's ability to distinguish organoid morphological differences, human brain organoids derived from healthy- or epilepsy- iPSCs (induced pluripotent stem cells) were embedded in 50% Matrigel® and imaged over 8 days (Figure 2B). Figure 2B illustrates that these cultures exhibited comparable growth (avg. area bar chart) but displayed distinct phenotypes (BF images). Morphology-related parameters tracking changes in object roundness (eccentricity) or brightness (darkness) were utilized to exemplify differential organoid phenotypes. Mature healthy organoids appeared darker and rounded (decreased eccentricity), while an increase in eccentricity was observed in patient organoids as they formed loose, disorganized aggregates (Figure 2B).

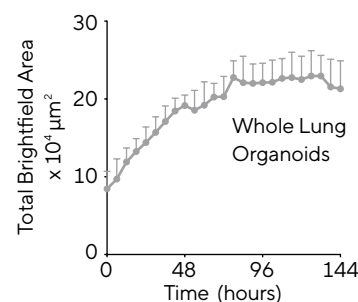
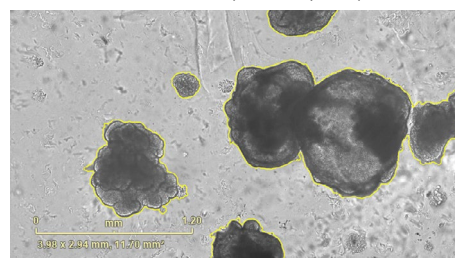
A. Intestinal Organoids Matrigel Dome (1:6 split)



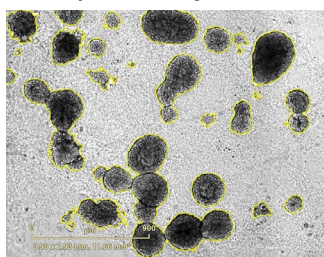
Hepatic Organoids Embedded No Base (2K cells/well)



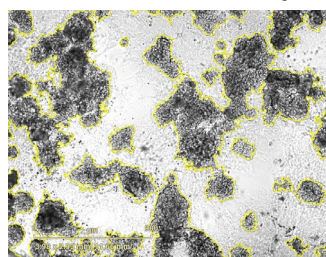
Lung Organoids Embedded With Base (2K cells/well)



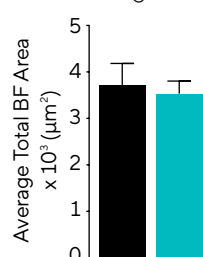
B. Healthy Brain Organoids



Patient-Derived Brain Organoids



Average Area



Darkness

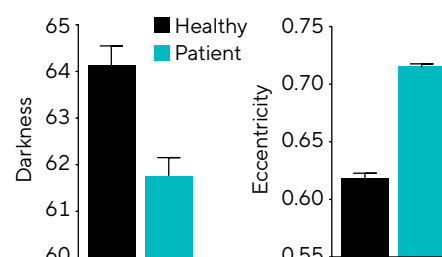


Figure 2: Acquisition and quantification of distinct organoid morphologies. Mouse intestinal (1:6 split, dome), hepatic (2K cells/well) and whole lung organoids (2K cells/well) were seeded (50% Matrigel®) into 96-well plates and imaged in an Incucyte®. Brightfield (BF) images (6 days post seeding) and time-course plots of the individual well total BF area (μm^2) over time (hours) show distinct organoid phenotypes and demonstrate cell type specific organoid growth, respectively (A). Healthy or diseased human brain organoids (2K cells/well) were embedded in 50% Matrigel® and imaged over 8 days. Images (6 days) and bar graphs demonstrate growth capabilities and differential phenotypes of healthy vs diseased organoids (B). All images captured at 4x magnification. Each data point represents mean \pm SEM, $n = 3 - 12$ wells.

Quantifying Organoid Growth and Death Over Time

To assess the impact of treatments on organoid growth and morphology, intestinal and hepatic organoid fragments were embedded in Matrigel® (50%) and allowed to form organoids for 3 days prior to treatment with protein kinase inhibitor staurosporine (1 µM, STP). Changes in organoid size and shape were kinetically monitored and quantified over time (4 - 10 days).

Time-courses and zoomed in BF images shown in figure 3B illustrate the effect of STP on hepatic organoid morphology. A concomitant increase in darkness and eccentricity was observed as STP induced cell death and elicited loss of distinctive rounded phenotype over time.

Figure 3A demonstrates that vehicle treated intestinal or hepatic organoids increase in size (10-fold or 3-fold respectively) and number (Figure 3B) over time while a marked reduction is observed in the presence of STP.

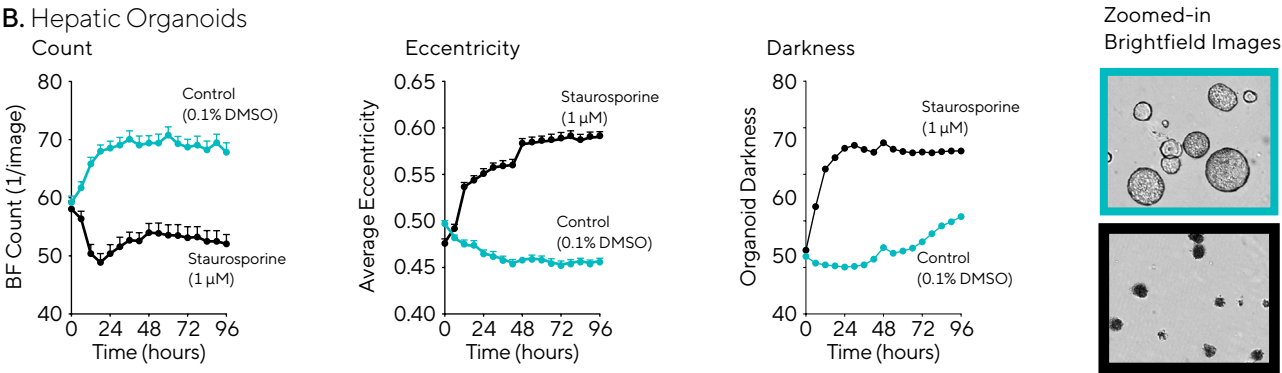
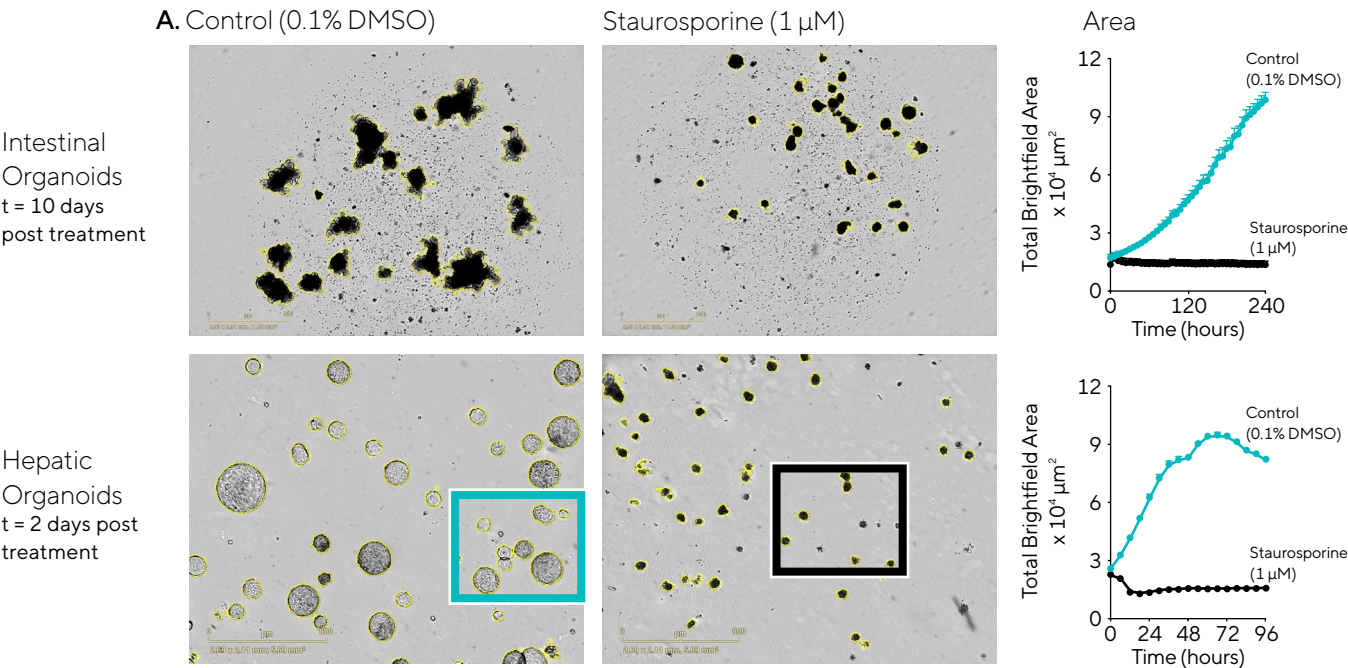


Figure 3: Perform automated label free quantification of organoids. Mouse intestinal (1:6 split) and hepatic fragments (1K cells/well) were embedded in Matrigel® (50%) in 96-well plates and allowed to form organoids for 3 days prior to treatment (vehicle or staurosporine; STP). Brightfield (BF) images (A) and corresponding time-courses of BF area (A) demonstrate the continued growth of vehicle treated organoids and the inhibitory effects of STP across both cell types. STP treated hepatic organoids lose distinctive rounded phenotype (increased eccentricity) and increase in darkness over time (B). Data were collected over a 96 - 240 hour period at 6 hour intervals. All images captured at 4x magnification. Each data point represents mean ± SEM, n=4 wells.

Probe Mechanisms of Action Using Real-Time Morphology Measurements

As patient-derived organoids (PDOs) retain the morphological and molecular characteristics of the tissue/tumour of origin, they are increasingly being used as *in-vitro* drug development models.¹ For these *in-vitro* drug studies, the ability to distinguish between cytotoxic and cytostatic cellular responses is crucial to establishing effective anticancer therapies.³ Performing multi-parametric quantitative measurements is key to understanding these dynamic drug responses.

To exemplify drug-specific changes in organoids, hepatic organoids were formed for 3 days and subsequently treated with staurosporine (STP, protein kinase inhibitor), cisplatin (CIS, DNA synthesis inhibitor) or fluorouracil (5-FU, thymidylate synthetase inhibitor). Concentration response curves (CRCs) representing the area under the curve analysis of total area, eccentricity, or darkness time-course data (0 – 96 hours) were then constructed to discriminate between cytotoxic and cytostatic agents (Figure 4).

All compounds caused a concentration dependent inhibition of organoid growth, yielding IC_{50} values of 3 nM for STP, 0.78 μ M for 5-FU and 9.7 μ M for CIS (area CRC, Figure 4).

However, while attenuation of organoid size was observed across all compounds, increases in eccentricity and darkness indicative of 3D structure disruption and cell death respectively were only observed in CIS and STP-treated organoids.

STP induced notable changes in organoid eccentricity across a range of concentrations (1.6 nM – 1 μ M, EC_{50} 0.5 nM) and evoked a concentration-dependent increase in organoid darkness (EC_{50} 53.3 nM), suggesting a strong cytotoxic mechanism of action (MoA). While concentration-dependent responses were also observed in CIS-treated organoids, substantially higher concentrations (50 – 100 μ M) were required to elicit comparable or greater effects on eccentricity (EC_{50} 32.5 μ M) or darkness (EC_{50} 31.7 μ M).

Conversely, 5-FU appeared to be more cytostatic, inhibiting organoid growth but not inducing cell death or disrupting distinct organoid phenotype. Differences between the size and morphology readouts support the cytostatic mechanism of 5-FU. Representative BF images confirm distinction between the cytotoxic MoA of STP and CIS and the cytostatic effects of 5-FU on hepatic organoids (Figure 4).

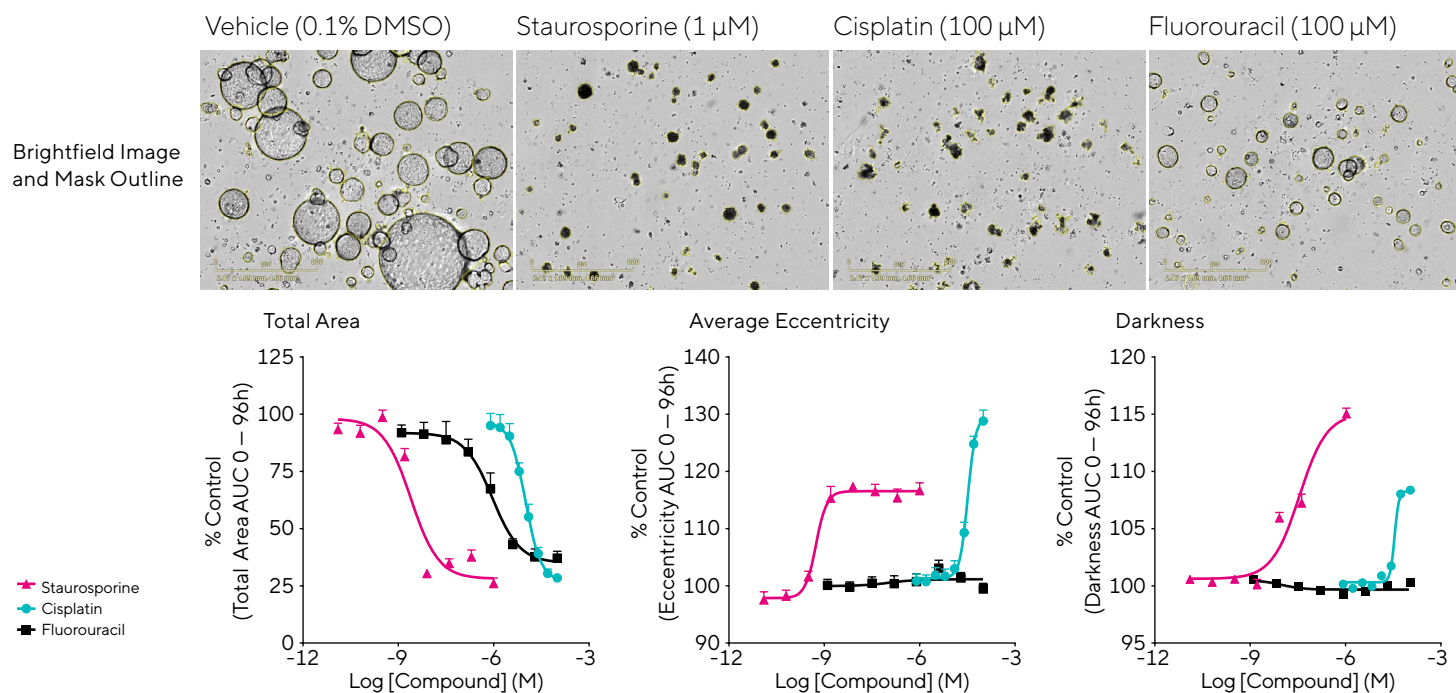


Figure 4: Distinguish between cytotoxic and cytostatic mechanisms of action using label-free measurements. Hepatic fragments were embedded (0.5K cells/well) in 50% Matrigel® and allowed to form organoids (3 days) prior to treatment. Brightfield images taken 2 day post treatment show compound-specific effects on organoid size and morphology. Concentration response curves (CRCs) of the area under the curve (AUC) analysis of area, eccentricity and darkness demonstrated differential profiles of cytotoxic (staurosporine and cisplatin) and cytostatic (fluorouracil) mechanisms of action. Data were collected over a 96-hour period at 6 hour intervals. Each data point represents mean \pm SEM, n = 3 separate test occasions.

Label-free Quantification of Forskolin-Induced Organoid Swelling

Cystic fibrosis (CF) is caused by mutations in the CFTR gene that severely reduce the function of the anion channel, cystic fibrosis transmembrane conductance regulator (CFTR). As disease expression is highly variable between patients (>1,900 CFTR mutations), effective responses to treatment therapies are challenging.^{4,5} Despite the promise of CFTR-specific drug therapies, the degree of individual CFTR function restoration has been limited by *in-vitro* screening models. However, numerous studies have recently highlighted the translational potential of organoids and demonstrated their use to successfully obtain patient-specific information on CFTR-modulator drug response.⁵

Here, we validate a rapid and label-free quantitative swelling assay for CFTR function in mouse intestinal organoids. Organoids formed for 3 days were treated with increasing concentrations of forskolin (Fsk; cyclic adenosine monophosphate inducing stimuli) and imaged in an Incucyte® every 15 – 20 minutes for up to 6 hours. Forskolin-induced swelling (FIS) was kinetically quantified by evaluating the percentage change in BF area (size) relative to the area at t = 0 hours.

Exposing intestinal organoids to forskolin caused a concentration-dependent increase in organoid size, while DMSO-treated organoids remained unchanged (Figure 5A and 5B). Note the 3-fold increase in size (6 hour post treatment) at the highest test concentration in comparison to control (Figure 5B). Additionally, as the lumen filled with fluid over time, stimulated organoids became more rounded and clearer, resulting in a reduction in eccentricity and darkness respectively (Figure 5C).

To demonstrate that FIS is CFTR-dependent and thereby mimicking the CF disease state, intestinal organoids were pre-incubated with CFTR inhibitor CFTR_{inh}-172 for 2 hours. The construction of concentration response curves revealed that swelling is CFTR-dependent as control organoids increased in size (>300% at 10 μ M Fsk), while treatment with CFTR_{inh}-172 reduced the FIS maximal response by >50% (~150% at 10 μ M Fsk, Figure 5D).

Validation data shown in figure 5 demonstrate the capability to kinetically visualise and quantify CFTR function label-free and illustrates the potential utility of this approach in cystic fibrosis drug development, diagnosis, or functional studies.

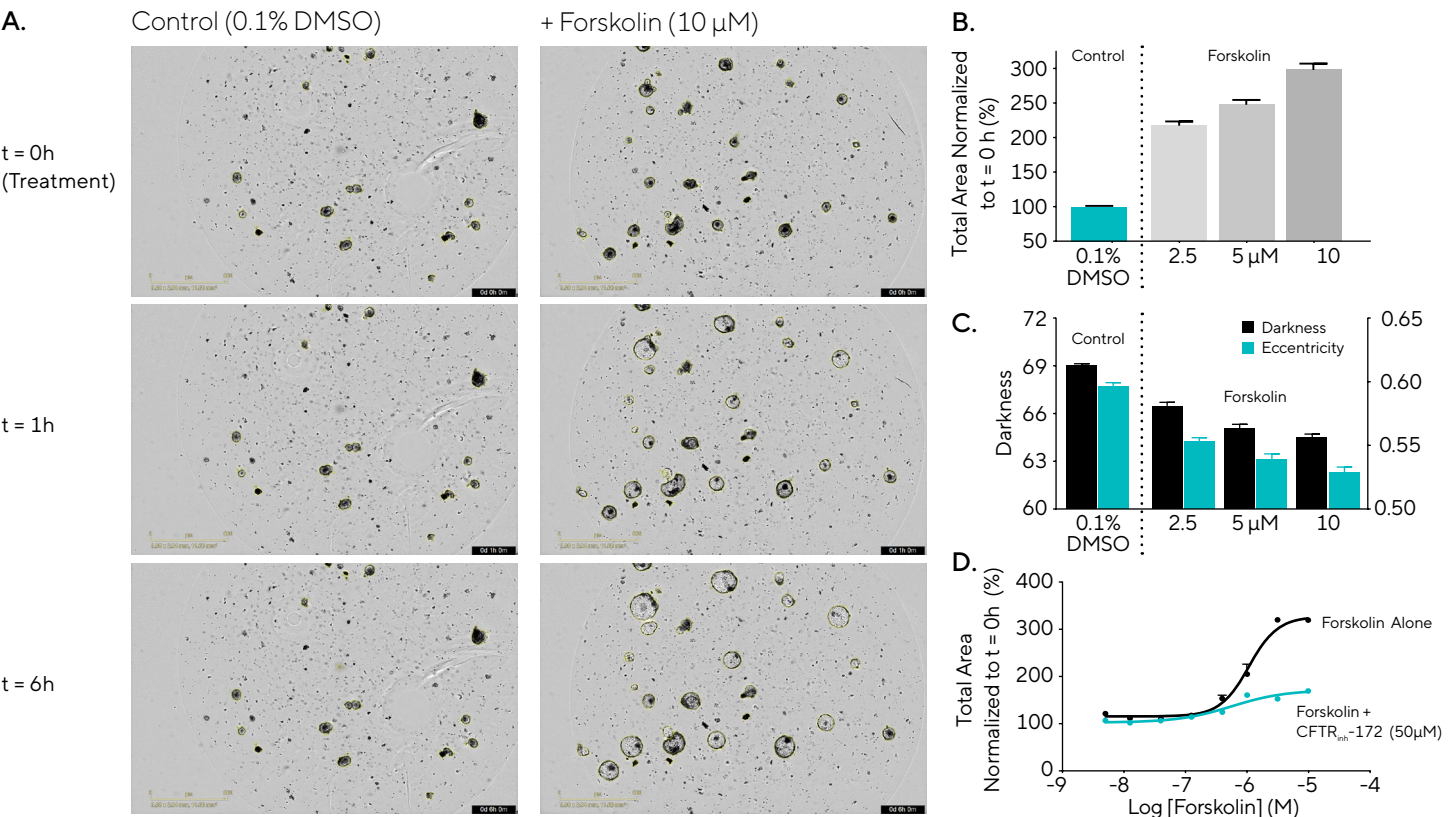


Figure 5: Quantify organoid swelling in response to Forskolin stimulation. Incucyte® brightfield (BF) images show effects of forskolin treatment on intestinal organoid (50% Matrigel® domes) size over time (A). Bar chart of BF area (total BF area normalized to t = 0 h) demonstrates that swelling is forskolin concentration-dependent (B). Following stimulation intestinal organoids exhibit a more rounded phenotype (decreased eccentricity) and clear lumen (decreased darkness) (C). Concentration response curve (CRC) of the area under the curve (AUC) analysis of area normalized to t = 0 hours (%) (0 – 6 hours) demonstrates that forskolin-induced swelling is cystic fibrosis transmembrane conductance regulator (CFTR)-dependent (D). Data were collected over a 6-hour period at 30 minute intervals. BF images captured at 4x magnification. Each data point represents mean \pm SEM, n=3.

Conclusion



In this application note, we demonstrate the use of the Incucyte® Live-Cell Analysis System, in combination with the Incucyte® Organoid Analysis Software Module, to simplify and facilitate temporal assessment of organoid growth or death. We have demonstrated:

- Automated software that can continuously locate and analyze embedded organoids in physiologically relevant conditions.
- The ability to kinetically visualize and quantify distinct organoid morphologies and segment individual objects embedded in Matrigel® across a range of cell types.
- The use of integrated, real-time label-free metrics to assess drug-induced cellular changes and characterize mechanisms of action in a 96-well plate format.
- Use of this approach to visualize and quantify CFTR function, thereby enabling label-free assessment of cystic fibrosis *in-vitro*.

References

1. I. H. H. C. Devanjali Dutta, **“Disease modeling in stem cell-derived 3D organoid systems,”** *Cell Press*, vol. 23, no. 5, pp. 393-410, 2017.
2. R. N. M. A. M. W. W. D. N. E. Y. S. Sandra L. Leibel, **“Generation of Complete Multi-Cell Type Lung Organoids From Human Embryonic and Patient-Specific Induced Pluripotent Stem Cells for Infectious Disease Modeling and Therapeutics Validation,”** *Current Protocols in Stem Cell Biology*, vol. 54, no. 118, pp. 1-10, 2020.
3. M. G. J. H. D. a. A. J. M. Shivaani Kummar, **“Drug development in oncology: Classical cytotoxics and molecularly targeted agents,”** *Br. J. Clin. Pharmacol.*, vol. 62, pp. 15-26, 2006.
4. J. M. B. C. K. v. d. E. Peter van Mourik, **“Intestinal organoids to model cystic fibrosis,”** *Eur. Respir. J.*, p. 54 : 1802379, 2019.
5. W. C. d. J. H. e. a. Dekkers JF, **“A functional CFTR assay using primary cystic fibrosis intestinal organoids,”** *Nat Med*, vol. 19, no. 7, pp. 939-945, 2013.

Intestinal organoids: a model to study the role of microbiota in the colonic tumor microenvironment

Harika Nalluri¹ , Subbaya Subramanian^{1,2} & Christopher Staley^{*,1,2,3} 

¹Department of Surgery, Division of Basic & Translational Research, University of Minnesota, Minneapolis, MN 55455, USA

²Masonic Cancer Center, University of Minnesota, Minneapolis, MN 55455, USA

³BioTechnology Institute, University of Minnesota, St. Paul, MN 55108, USA

*Author for correspondence: Tel.: +1 612 625 8831; cmstaley@umn.edu

Colorectal cancer (CRC) is the third most common cause of cancer worldwide. Recent studies have suggested that a dysbiotic shift in the intestinal microbial composition of CRC patients influences tumorigenesis. Gut microbes are known to be integral for intestinal homeostasis; however, the mechanisms by which they impact CRC are unclear. Further knowledge about these complex interactions may guide future CRC management. Thus, it is crucial to establish high-quality experimental models to understand the relationship between host, tumor, microbiota and their metabolic interactions. In this review, we highlight the significance of intestinal microbiota and their metabolites in CRC, challenges with current experimental models, advantages and limitations of organoid culture and future directions of this novel model system in CRC-associated microbiome research.

First draft submitted: 23 December 2019; Accepted for publication: 19 October 2020; Published online: 20 November 2020

Keywords: 3D model • colorectal cancer • microbial metabolites • microbiota • organoid • tumoroid

Background

Significant progress in colorectal cancer (CRC) research has highlighted the importance of the tumor microenvironment (TME) in tumor development. Intestinal microbiota and associated metabolites have been implicated as key members of this tumor milieu, affecting CRC tumorigenesis, host metabolism and immunity [1]. High-throughput DNA sequencing has led to considerable advances in our understanding about the role of these microbes on a compositional level, but their functional roles on a mechanistic level remain largely undefined. Current experimental models are limited in their disease modeling capacity and would benefit from additional innovative systems that could further our knowledge in this field. More accurate understanding of how different microbes affect tumor growth will ultimately guide the creation of novel therapies to treat CRC in the future.

Intestinal microbiota in CRC

Both genetic and environmental factors contribute to the etiology of CRC. The adenoma–carcinoma sequence refers to the multistep progression of genetic mutations by which most colorectal tumors arise. Other factors that influence the risk of CRC include history of inflammatory bowel disease, obesity, diet, lifestyle – and more recently identified – gut microbiota [2]. The human GI tract harbors trillions of microorganisms that constitute the gut microbiota. Prominent bacterial populations in healthy adults include Gram-positive *Firmicutes* and Gram-negative *Bacteroidetes*, while other phyla exist at lower abundances [3].

Recent studies have identified alterations in the gut microbial compositions of CRC patients that are postulated to influence the development of cancer [4]. Specifically, CRC patients have been shown to have an overall decrease in bacterial diversity in comparison to healthy patients [5]. They have also been found to have greater abundances of specific species including *Fusobacterium nucleatum*, enterotoxigenic *Bacteroides fragilis*, *Escherichia coli* and *Enterococcus faecalis* [6].

Several of these bacteria engage host pathways that can contribute to tumorigenesis. For example, Rubinstein *et al.* demonstrated that *F. nucleatum* stimulates proliferation of CRC via expression of FadA adhesin in both cell culture and xenograft mice [7]. FadA binds to E-cadherin that activates β -catenin, and promotes expression of oncogenes, transcription factors, and growth of CRC cells. Additionally, enterotoxigenic *B. fragilis* has also been shown to activate the β -catenin pathway via *B. fragilis* toxin in human colonic cell lines and *Apc^{min/+}* mice [8,9]. In contrast, other commensal bacterial species have been found to have antitumor effects. Lee *et al.* showed that *B. adolescentis* stimulates macrophage activation and production of pro-inflammatory cytokines (i.e., TNF- α) that are cytotoxic to tumor cells and inhibit proliferation of human CRC cell lines [10]. Thus, it is apparent that intestinal microbes can significantly influence CRC growth; however, a detailed understanding of their mechanistic involvement in the TME remains an active area of study.

Microbially derived metabolites

Ultimately, the impact of gut microbiota on CRC tumorigenesis is largely driven by the cumulative effects of their metabolic products. Undigested dietary compounds are metabolized by resident microbiota to produce a wide range of metabolites. Given that their potential roles in CRC have been recently reviewed [11], selected major metabolic pathways will be highlighted.

Three significant products of carbohydrate fermentation include the short-chain fatty acids (SCFAs) acetate, propionate and butyrate. They have important immunomodulatory and anti-inflammatory effects, for instance, via regulation of histone acetylation and modulation of colonic Treg cells [12]. Butyrate is the main energy source of colonocytes, and thus has been studied extensively. However, there is conflicting evidence regarding its role in CRC tumorigenesis. Greater concentrations of butyrate have been found in the stool of healthy individuals when compared with CRC patient stool [13]. The butyrate receptor GPR109a, encoded by *NIACR1*, has been associated with blockade of the protumorigenic NF- κ B and selective apoptosis of CRC in human colonic cell lines [14]. It has also been shown to stimulate an anti-inflammatory response by increasing differentiation of Treg cells and IL-10-producing cells. When the *NIACR1* gene was knocked out, increased susceptibility to colon cancer was observed in a murine model [15]. In contrast, Belcheva *et al.* showed that butyrate stimulates proliferation of aberrant colon epithelial cells in *Msh2*-deficient mice, leading to increased polyp formation [16].

Secondary bile acids represent another class of metabolites produced by intestinal microbiota that may impact CRC tumorigenesis. Roughly 5% of taurine or glycine-conjugated primary bile acids evade the enterohepatic circulation and are converted to secondary bile acids via bile salt hydrolases produced by intestinal microbes [17]. These compounds are suggested to promote cancer progression via stimulation of reactive oxygen species, inhibition of apoptosis and enhancement of cancer cell proliferation [18]. For example, Cao *et al.* found that treatment of *Apc^{min/+}* mice with deoxycholate increased intestinal tumor formation via enhanced Wnt signaling and decreased apoptosis of tumor cells [19].

Current state of CRC mouse models

Much of the current literature regarding the impact of gut microbiota on CRC has been conducted with 2D cell lines or murine animal models. Although these models generate valuable information, they have limitations in their suitability for clinical translation. A study investigating Phase I cancer drug trial outcomes showed that only 3.8% of patients had a clinically significant response from drugs that worked in mouse models [20]. Hence, there is still much incongruity between induced tumors studied in mouse models and spontaneous tumors that arise in humans.

Genetically engineered mouse models

Genetically engineered mouse models (GEMMs) are established by altering the genome of mice with specific mutations known to cause CRC. One of the most widely used GEMM in CRC-associated microbiome research is *Apc^{min/+}*, a analog for familial adenomatous polyposis syndrome [21]. Many other GEMMs have also helped guide this field, including models of hereditary nonpolyposis CRC (i.e., *Msh2^{-/-}*) and those that use the Cre-*loxP* system to restrict tumor formation to tissues of interest [22]. Nonetheless, these models are limited because they are costly, time and labor intensive, and they do not imitate the formation of sporadic tumors in humans [23]. Selected genes are activated in all cells of a particular tissue rather than a genetic mutation initiated at the single cell level. This can cause widespread tumor formation throughout the intestine, including the small bowel, and can lead to high tumor burden that limits metastatic potential [24].

Chemically induced mouse models

Chemically induced mouse models involve exposure of mice to carcinogens, such as azoxymethane and dextran sodium sulfate, where inflammation drives cancer. These models are frequently used in CRC-associated microbiome studies [25]. However, it should be noted that incidence of tumor development depends on the type of carcinogen used, dosage, frequency and route of administration. Sensitivity to carcinogens can also be affected by the age, sex and genetic background of mice [26]. The chemical itself may alter commensal gut microbiota prior to onset of colitis [27]. Other limitations include differences in mutation sequence compared with humans, low incidence of neoplastic transformation and poor metastatic potential [28,29]. Finally, these models are used to study colitis-associated cancer, which represents a small subgroup of individuals, rendering them less translatable to most CRC patients.

Transplantation mouse models

There are several different transplantation mouse models of CRC including allograft and xenograft models in which cell lines are injected either subcutaneously or orthotopically. Cell line and patient derived xenograft models have provided critical insights into cancer biology and drug development [30]. Unfortunately, these models are inefficient for high-throughput screens and can require 4–8 months before mice can be used [31]. Also, engraftment rates can vary, especially depending on tumor aggressiveness, resulting in selection bias with some human cancer phenotypes represented more than others [32]. Orthotopic transplantation allows for the study of site-specific interactions; however, this method can be expensive and labor intensive [31]. Another issue is that many of these models use immune-deficient mice, which can significantly impact how tumors behave. Some have attempted to address this by developing mice with humanized immune cell lineages [33]. However, these models still frequently show variable responses to immune mediators compared with humans.

Introduction of a 3D model system

Although current disease modeling systems to study the CRC-associated microbiome are extremely important, their translational value should be enhanced with emerging approaches. Advances in stem cell biology have led to the development of 3D *in vitro* systems. The term ‘organoid’ has been used to describe different types of 3D cell aggregates. This definition has been refined over time to describe complex, self-organizing 3D structures grown from multipotent stem cells that display functional and architectural similarities to *in vivo* organs [34]. Organoids can be derived from either pluripotent (embryonic or induced pluripotent stem cells) or adult (tissue-specific) stem cells. While pluripotent stem cells have been used with *in vitro* culture systems for decades [35], adult stem cells have previously been considered to have limited proliferation potential.

Sato *et al.* published the most widely used method to generate organoids with adult Lgr5⁺ stem cells from murine intestinal crypts [36], and subsequently, from human intestinal crypts [37]. In this system, stem cells are grown in Matrigel, a laminin-rich extracellular support matrix, with a set of growth factors that mimic the *in vivo* crypt base microenvironment. Within 2 weeks, they form 3D structures with a central lumen lined by villus-like epithelium and crypt-like domains. They display multilineage differentiation involving all intestinal cell types, including absorptive enterocytes, antimicrobial Paneth cells, hormone-producing enteroendocrine cells and mucus-producing goblet cells. Organoids provide a novel way to study gut microbiota and CRC in a 3D *in vitro* culture system that allows for a wide range of basic and translational applications.

3D architecture

Organoid cultures mimic *in vivo* epithelial development, with differentiated cells that migrate along a crypt–villus axis [36]. They exhibit a near-physiological environment for epithelial cells to grow and participate in cell–cell and cell–matrix interactions. This is important because the architecture of a cell population largely affects how cells interact with one another and with the surrounding extracellular matrix. Some examples of how organoids imitate natural cellular interactions include expression of tight junctions, production of mucus, cytokine signaling and maintenance of apical-basal polarity [38]. Additionally, the 3D nature of organoids allows for a mixture of oxygen and nutrient-rich areas as well as necrotic and hypoxic regions, as would occur *in vivo* [39]. These features enhance the physiologic relevance of the organoid model to study interactions between colonic epithelial cells, gut microbiota and metabolites.

Table 1. Intestinal organoids to study gut microbes.

Method of coculture	Microbes	Additional cells	Ref.
Microinjection	<i>B. thetaiotaomicron</i>		[53]
	<i>pks⁺ E. coli</i>		[54]
	Commensal <i>E. coli</i> and pathogenic <i>E. coli</i> O157:H7	PMNs	[55]
Incubation in media	<i>L. rhamnosus</i> GG, <i>L. paracasei</i> , <i>B. bifidum</i>		[52]
	<i>Akkermansia muciniphila</i> , <i>Faecalibacterium prausnitzii</i>		[56]
	<i>L. reuteri</i> D8, <i>L. acidophilus</i>	Lamina propria lymphocytes	[57]

PMN: Polymorphonuclear leukocyte.

Tumoroids

Organoids prepared with isolated tumor cells from cancerous tissues are known as ‘tumoroids’. They form 3D sphere-like structures comprised of tumor epithelial cells. They are becoming a valuable tool in cancer research and have been established for multiple cancer types including colorectal, breast, prostate, pancreatic, liver and stomach cancers [40]. CRC research has been limited by traditional 2D culture techniques that lack tumor heterogeneity, with polyclonal populations that become multi or monoclonal over time [41]. CRC tumoroids, on the other hand, exhibit remarkable similarity to their primary tumors, with histologic resemblance and maintenance of intratumor heterogeneity and mutational diversity [42,43]. Organoids can also be genetically modified with either viral gene transfer, liposomal transfection or electroporation [44]. There are many examples of how gene-editing technologies such as shRNA or CRISPR/Cas9 have been used in this model, which have been well summarized elsewhere [45].

Modeling host–microbe interactions

Use of organoids to model host–microbe interactions is an evolving field. A variety of microbes including *Helicobacter pylori*, *Salmonella enterica*, *E. coli*, rotavirus and *Plasmodium* spp. have been studied with this culture system, and this has been reviewed thoroughly elsewhere [46–48]. Introduction of microorganisms to organoids can be facilitated by a variety of approaches including disruption of organoids into single-cell suspensions, polarization to 2D monolayers or microinjection into the apical lumen of intact organoids [49].

Currently, host–microbe relationships are primarily studied with 2D cell cultures or animal models. However, certain microbes that infect humans do not grow in these conditions. For example, human norovirus, a common cause of diarrhea, does not infect gastrointestinal epithelial cells in cell culture or in mice due to a lack of species specificity. Yet, Ettayebi *et al.* was able to cultivate multiple human norovirus strains in enterocytes within human intestinal enteroid monolayer cultures, demonstrating that this *in vitro* culture system has crucial elements that allow for the growth of certain microorganisms [50].

The 3D architecture of organoids also allows for the study of anaerobic bacteria, which has been difficult to do with 2D cell lines. Leslie *et al.* showed that pathogenic *Clostridium difficile* was viable for up to 12 hours after injected into intestinal organoids [51]. This validates that organoids have low intraluminal oxygen concentrations suitable for the growth of anaerobic bacteria, regardless of exposure to ambient oxygen.

Intestinal microbes

There are several examples of how intestinal organoids could be used to study gut microbes, shown in Table 1. For instance, Aoki-Yoshida *et al.* found that culturing intestinal organoids with *Lactobacillus rhamnosus* increased Toll-like receptor 3 mRNA levels, important for the innate immune response [52]. This did not occur when organoids were exposed to *L. paracasei* and *Bifidobacterium bifidum*. Engevik *et al.* focused on the Na⁺/H⁺ exchanger 3 (NHE3), which plays a key role in intestinal Na⁽⁺⁾ absorption. They inoculated *B. thetaiotaomicron* in wild-type and NHE3-deficient terminal ileum organoids to identify how loss of NHE3 alters the microbial landscape of the intestine [53].

Although studies using organoids to examine intestinal microbes in the setting of CRC are scarce, lately there have been some compelling uses of this novel system. In a recent publication, researchers used organoids to study the role of *pks⁺ E. coli* in the CRC tumorigenesis [54]. These bacteria produce colibactin, which has been suggested to contribute to CRC via DNA damage and chromosomal instability. After healthy human intestinal organoids were injected with *pks⁺ E. coli* over 5 months, whole-genome sequencing revealed a distinct mutational signature that has also been seen in a subset of human CRC genomes.

Microbial metabolites

In addition to modeling host–microbe interactions, organoids have shown promise in studying the role of microbial metabolites. Lukovac *et al.* showed that exposure of murine intestinal organoids to supernatant from *A. muciniphila* and *F. prausnitzii* monocultures, as well as to individual butyrate, propionate and acetate solutions produced differential changes in expression of genes involved in cellular growth and regulation of metabolic pathways [56]. Another study that cultured SCFAs with intestinal organoids found that butyrate, in contrast to other SCFAs, upregulates *ALDH1A3* expression via histone deacetylase 3 inhibition, important for the epithelial conversion of retinol to retinoic acid [58]. Park *et al.* also showed that coculture of murine intestinal organoids with SCFAs led to an increase in epithelial cell turnover, confirming results seen in a mouse model [59].

Kaiko *et al.* took advantage of the distinctive ability of adult stem cell-derived organoids to differentiate to specific cell types based on culture conditions to make enriched cultures of colonocytes [60]. They analyzed the effect of 92 bacterial metabolites and pathogen-associated molecular patterns, concluding that butyrate suppresses the proliferation of intestinal stem cells but not differentiated colonocytes. The researchers hypothesized that the crypt architecture forms a metabolic barrier, protecting stem cells from luminal butyrate that is metabolized by overlying colonocytes. Organoids have also been used to identify how other dietary compounds affect epithelial homeostasis and tumorigenesis. For instance, Toden *et al.* highlighted the antitumorigenic properties of oligomeric proanthocyanidins (metabolites present in certain fruits and vegetables) in patient-derived CRC tumor organoids [61].

Incorporating other members of the TME

Tumor growth relies on the complex interplay between neoplastic cells and components of the TME. In addition to gut microbiota, this includes the extracellular matrix, as well as stromal cells like immune cells, fibroblasts and endothelial cells [62]. Understanding the mechanisms by which host immune and inflammatory responses alter the composition of this microenvironment is paramount in cancer research. Unfortunately, the differences between human and murine immune systems likely contribute to phenotypic variances seen with experimental mouse models, rendering them less translatable. Alternatively, organoids allow for the study of species-specific interactions with human-derived 3D cell cultures that can be fine-tuned with coculture techniques to recapitulate the TME. Many different cell types have been cocultured with organoids, as illustrated in Figure 1.

Immunity

The mucosal barrier function of intestinal epithelial cells consists of physical barriers, like tight junctions, and chemical barriers, such as release of cytokines and chemokines that activate the immune response. Immune cells including intra-epithelial lymphocytes (IELs) and macrophages preserve and enhance this mucosal barrier integrity and contribute to overall gut homeostasis [63]. While few have cocultured intestinal organoids with these cell types to examine their role in tumorigenesis, the feasibility of such a study is supported by several coculture studies.

For instance, Rogoz *et al.* showed that activated peripheral T cells cocultured with murine enteroids proceeded to develop many characteristics of IELs, proving that this system can be used to study T-cell survival and differentiation [64]. Previous studies showed that the *in vitro* life span of isolated IELs without cytokine supplementation was limited to 48 hours. However, Nozaki *et al.* identified survival of IELs three days after coculture with murine enteroids, which was further maintained for a period of 2 weeks after addition of IL-2, -7 and -15 to the growth media [65]. They also used time lapse fluorescent imaging to verify active movement of IELs along the basolateral surface of intestinal epithelial cells.

To study the regulatory effect of microbiota on gut mucosal barrier function, Hou *et al.* cultured murine intestinal organoids with lamina propria lymphocytes [57]. Addition of *L. reuteri* D8 increased proliferation of organoids and improved their recovery after TNF- α -induced damage. Noel *et al.*, investigating the role of macrophages in gut barrier function, found that human monocyte-derived macrophages cocultured with enteroid monolayers recapitulated *in vivo* cytokine signaling and response to infection [66]. After addition of enterotoxigenic and enteropathogenic *E. coli*, macrophages facilitated bacterial clearance with phagocytic activity and enhanced barrier function.

Microbial metabolites have also been studied in this context. Several *Peptostreptococcus* spp. have been shown to metabolize tryptophan to indoleacrylic acid, which promotes intestinal barrier function and attenuates inflammatory responses. Włodarska *et al.* created a coculture system of murine colonic organoids and bone marrow-derived macrophages, which were treated with a variety of metabolites followed by stimulation with lipopolysaccharide

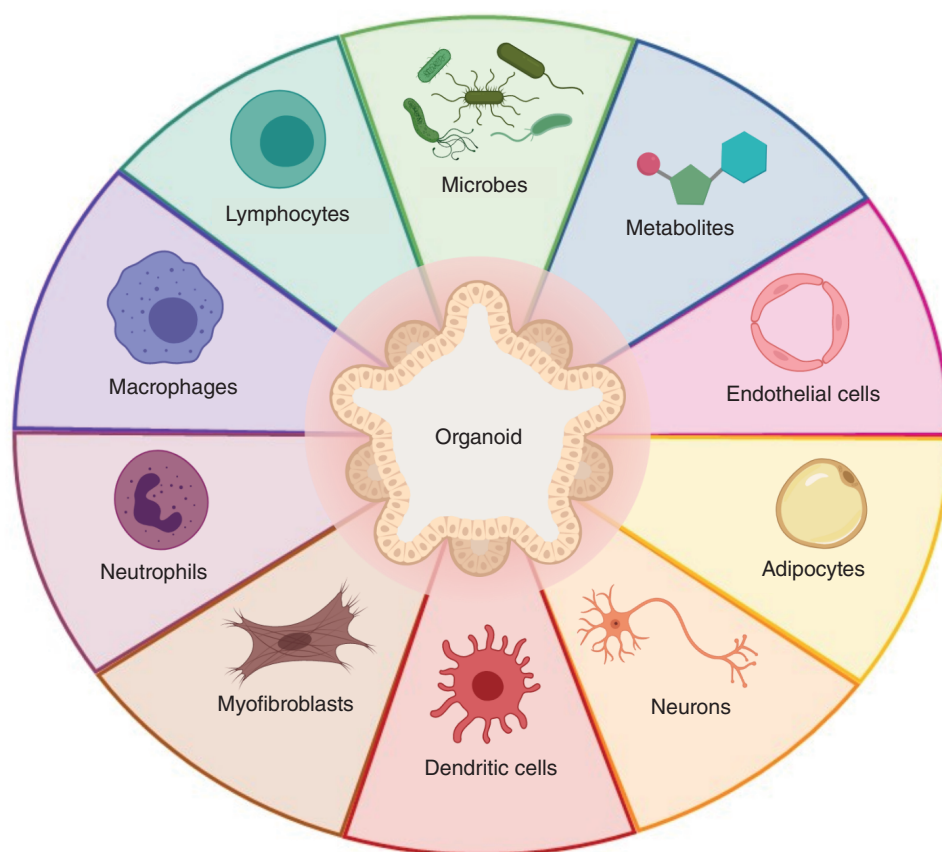


Figure 1. Coculture intestinal organoids to reconstruct the tumor microenvironment.
Image made with BioRender.com.

(LPS) [67]. The indoleacrylic acid-treated cocultures had enhanced expression of *MUC2* and *IL10* and reduced expression of *TNF*.

Organoid coculture techniques have also been used to study other key members of the immune response such as neutrophils. Karve *et al.* cocultured neutrophils with induced human intestinal organoids to examine host response to infection with different strains of *E. coli* [55]. Commensal *E. coli* did not cause damage, whereas *E. coli* 0157:H7 led to increased stress response via production of reactive oxygen species, upregulation of inflammatory mediators like IL-8 and migration of neutrophils from the organoid margin to the inside of their lumen.

Inflammation

Inflammation is a noteworthy driver of cancer that promotes tumor initiation, growth and progression [68]. Inflammatory signals can modulate the TME by recruiting and reprogramming stromal cells, such as fibroblasts and endothelial cells, to support tumor growth. Organoids have become a useful model to more precisely identify how these surrounding cells may affect intestinal physiology, which will be important for the future of CRC-associated microbiome research.

For instance, intestinal subepithelial myofibroblasts have been recognized as important supportive cells in the intestinal stem cell niche. The growth of both human and murine enteroids were enhanced when grown on top of a confluent monolayer of intestinal subepithelial myofibroblasts [69,70]. Intestinal myofibroblasts also improved the viability of murine intestinal crypts in a multilayer organotypic cell culture performed in a Transwell® permeable

support (Corning Inc., NY, USA) [71]. Similarly, dendritic cells have been found to participate in the intestinal stem cell niche by activating Notch signaling in *Lgr5*⁺ cells through direct physiological contact when cocultured with murine intestinal organoids [72].

Nerve fibers have also been implicated in the regulation of the intestinal stem cell niche and support of carcinogenesis. Westphalen *et al.* established a coculture system of gastrointestinal organoids with primary neurons isolated from the spinal cord of mice and found that a subset of tuft cells, argued to have a role in inflammation-induced carcinogenesis, could only survive in the presence of nerves [73]. Additionally, accumulation of mesenteric fat has been proposed to trigger local inflammatory signaling. Coculture of intestinal organoid monolayers with differentiated adipocytes in a Transwell[®] induced pro-inflammatory genes in both cell types, supporting direct inflammatory crosstalk [74].

Blood vessels, which are important for intestinal function and cancer progression, have been difficult to introduce into organoid cultures. However, advances in microfluidic technology have led to the development of ‘organoids-on-a-chip’. Kasendra *et al.* used such a device, with two microchannels separated by a microporous membrane, to coculture human intestinal epithelial cells dissociated from organoids with intestinal microvascular endothelial cells [75]. This novel platform permits physiologic fluid flow and vascularization of organoids.

An emerging preclinical model

As we uncover the utility of the organoid culture system, its application as a preclinical model has become apparent. Organoids preserve tissue identity on a genetic level over time, strengthening their capacity for disease modeling and long-term clonal expansion. They expand the ability to study nuanced molecular variations in individual tumor profiles and rare cell lineages from limited starting material, enabling their use in high-throughput research [76].

Drug discovery

In this emerging field of microbiome research, gut microbiota modulation has been suggested as a potential strategy to prevent and treat CRC. Therapies such as probiotics, antibiotics and fecal microbiota transplantation have been proposed as options to modify gut microflora composition [77]. The organoid system provides a novel platform to study these experimental therapies in biologically representative samples. It also offers the opportunity to perform large-scale repetition of experiments. High-throughput, automated platforms have been established to perform drug assays with organoids grown in 384-well format [78,79]. Microengineered systems, such as organoids-on-a-chip, also permit high-throughput manipulation and analysis of organoids, rendering them more controllable constructs for drug testing [80].

Precision medicine

To account for individualized host responses to gut microbiome intervention, personalized microbiome therapy may be critical for successful clinical treatment [77]. The ability to culture and cryopreserve healthy and cancerous human organoids enables the establishment of CRC tumoroid ‘biobanks’ derived from patient tissue. Development of tumoroid libraries is still in the early stages, but they have tremendous potential for advancing personalized therapy [81–83]. For instance, van de Wetering *et al.* established an organoid biobank of matched malignant and healthy tissue from 18 patients and studied their response to 83 different compounds, including experimental drugs, agents in clinical trial and current chemotherapeutics [81]. They examined the mutational profiles of the original tissue specimens to interpret drug responses of groups of organoids with similar driving mutations. Ultimately, organoids could contribute greatly to the future of precision medicine. However, further studies will be needed to determine the validity of using patient-derived tumoroids to predict clinical drug responses and create individualized therapies.

Limitations

As with any model system, there are limitations to organoid culture that must be addressed. First, there is a lack of standardization among organoids that limits their potential for reproducibility. Consistent size, shape and cellular composition of organoids cannot be guaranteed [84]. This can also lead to potential difficulties with quantification. When organoids have more dying cells within their lumen, they appear darker and more loosely packed. Some current assays measuring cell viability and death rely on user-dependent manual observations using brightfield microscopy or staining techniques that are limited by extracellular matrix properties [85]. Advances in functional assays and single-cell analysis techniques will be needed to characterize organoid features more thoroughly.

Properties of extracellular matrix, such as matrix stiffness, have also been found to alter organoid proliferation [86]. These components should be considered because they could also potentially affect drug penetrance and efficacy. Additionally, growth factors added to culture medium may lead to selective growth of certain subclones of the parent tumor, which could result in bias that may not be seen *in vivo*. Drost *et al.* made use of this by removing specific growth factors to functionally select for certain clonal mutant organoids [87].

Although some have observed that tumoroids can remain genetically stable over time, the potential for clonal divergence cannot be dismissed given the genetic instability of many CRCs [88]. Potential gene expression differences may exist after prolonged culture, and further studies exploring long-term clonal dynamics after numerous passages are needed.

Despite advances in coculture techniques, the complex TME present *in vivo* is not easy to replicate in cell culture. This is a limitation to any *in vitro* model, and organoids are not exempt from this. A paucity of normal directional cues from the body can create some unavoidable differences seen experimentally. Ongoing experimentation in coculture and incorporation of microfluidics systems will be needed to introduce other vital TME components [89].

Finally, coculture techniques, such as microinjection, may be resource intensive and technically difficult to perform. New high-throughput, semi-automated platforms may make the organoid lumen more accessible [90]. These potential limitations will need further investigation as researchers continue to work with this culture system.

Conclusion

Organoids will serve as a key bridge between traditional 2D cell cultures and *in vivo* mouse models. They are physiologically relevant and offer many basic and translational opportunities to study gut microbiota in CRC. They can be modified and cocultured with other members of the tumor milieu in a controlled environment, and provide a high-throughput platform to study novel therapies. As organoid technology continues to evolve, it is feasible that this culture system could contribute to significant advances in CRC-associated microbiome research.

Future perspective

It is exciting to consider that organoids could expand opportunities to further comprehend the relationship between the human gut microbiota and CRC. Another powerful aspect about the evolution of organoid technology is the ability to transplant organoids into *in vivo* models. Scientists have already begun to explore a few different ways to transplant organoids into mice to create a more accurate CRC murine model.

O'Rourke *et al.* used noninvasive rectal enemas after pretreatment with dextran sulfate sodium to engraft mice with intestinal tumoroids, allowing tumor growth in the epithelium similar to human CRC [91]. Roper *et al.* performed orthotopic injections of gene-edited CRC tumoroids into the submucosal layer of the murine colon, without needing to injure the entire colon [92]. Others have transplanted intestinal organoids into murine kidney capsules or mesentery [93–96]. Many of these models exhibited development of tumors that eventually metastasized to the liver, providing optimism for a new metastatic murine model of CRC.

Author contributions

H Nalluri drafted the manuscript. S Subramanian and C Staley edited and contributed to the manuscript. All authors have read and approved the final manuscript.

Financial & competing interests disclosure

H Nalluri was supported, in part, by the Hubbard Broadcasting Foundation. The authors have no other relevant affiliations or financial involvement with any organization or entity with a financial interest in or financial conflict with the subject matter or materials discussed in the manuscript apart from those disclosed.

No writing assistance was utilized in the production of this manuscript.

Executive summary

Colorectal cancer & gut microbiota

- Colorectal cancer (CRC) has been linked to a dysbiotic shift in gut bacterial community composition. Intestinal microbes and their metabolites have been found to influence tumorigenesis, and these pathways need further investigation.

CRC mouse models

- Current mouse models have limited translational capacity due to interspecies variations and minimal opportunity for manipulation of niche components.

Organoid culture system

- Organoid cultures are 3D *in vitro* systems that are highly adaptable and resemble intestinal epithelium with similar physiology, shape and cell makeup.

Organoids to study microbes

- Organoids can be useful for modeling host–microbe interactions and have been used to study a variety of microbes and metabolites.

Tumor microenvironment

- Components of the tumor milieu can be incorporated into organoid cultures to study tumor development in a relevant environment.

Preclinical model

- Organoids provide a high-throughput platform to study novel therapies in a patient specific fashion.

Limitations

- Organoids have some limitations that will require further examination including growth variability, difficulty with quantification and potential impact of extracellular matrix or growth factors.

Future perspective

- Organoid transplantation into mice may represent a new *in vivo* metastatic model of CRC.

References

1. Garrett W. Cancer and the microbiota. *Cancer Immunol. Immunother.* 348(6230), 80–86 (2015).
2. Kuipers EJ, Grady WM, Lieberman D *et al.* Colorectal cancer. *Nat. Rev. Dis. Prim.* 1(1), 15065 (2015).
3. Ley RE, Hamady M, Lozupone C *et al.* Evolution of mammals and their gut microbes. *Science* 320(5883), 1647–1651 (2008).
4. Maisonneuve C, Irrazabal T, Martin A, Girardin SE, Philpott DJ. The impact of the gut microbiome on colorectal cancer. *Annu. Rev. Cancer Biol.* 2(1), 229–249 (2018).
5. Ahn J, Sinha R, Pei Z *et al.* Human gut microbiome and risk for colorectal cancer. *J. Natl Cancer Inst.* 105(24), 1907–1911 (2013).
6. Saus E, Iraola-Guzmán S, Willis JR, Brunet-Vega A, Gabaldón T. Microbiome and colorectal cancer: roles in carcinogenesis and clinical potential. *Mol. Aspects Med.* 69, 93–106 (2019).
7. Rubinstein MR, Wang X, Liu W, Hao Y, Cai G, Han YW. *Fusobacterium nucleatum* promotes colorectal carcinogenesis by modulating E-cadherin/ β -catenin signaling via its FadA adhesin. *Cell Host Microbe* 14(2), 195–206 (2013).
8. Wu S, Morin PJ, Maouyo D, Sears CL. *Bacteroides fragilis* enterotoxin induces c-Myc expression and cellular proliferation. *Gastroenterology* 124(2), 392–400 (2003).
9. Wu S, Rhee K-J, Albesiano E *et al.* A human colonic commensal promotes colon tumorigenesis via activation of T helper type 17 T cell responses. *Nat. Med.* 15(9), 1016–1022 (2009).
10. Lee DK, Jang S, Kim MJ *et al.* Anti-proliferative effects of *Bifidobacterium adolescentis* SPM0212 extract on human colon cancer cell lines. *BMC Cancer*. 8(310), 1–8 (2008).
11. Louis P, Hold GL, Flint HJ. The gut microbiota, bacterial metabolites and colorectal cancer. *Nat. Rev. Microbiol.* 12(10), 661–672 (2014).
12. Smith PM, Howitt MR, Panikov N *et al.* The microbial metabolites, short-chain fatty acids, regulate colonic Treg cell homeostasis. *Science* 341(6145), 569–573 (2013).
13. Weir TL, Manter DK, Sheflin AM, Barnett BA, Heuberger AL, Ryan EP. Stool microbiome and metabolome differences between colorectal cancer patients and healthy adults. *PLoS ONE* 8(8), e70803 (2013).
14. Thangaraju M, Cresci GA, Liu K *et al.* GPR109A is a G-protein-coupled receptor for the bacterial fermentation product butyrate and functions as a tumor suppressor in colon. *Cancer Res.* 69(7), 2826–2832 (2009).
15. Singh N, Gurav A, Sivaprakasam S *et al.* Activation of the receptor (Gpr109a) for niacin and the commensal metabolite butyrate suppresses colonic inflammation and carcinogenesis. *Immunity* 40(1), 128–139 (2014).
16. Belcheva A, Irrazabal T, Robertson SJ *et al.* Gut microbial metabolism drives transformation of MSH2-deficient colon epithelial cells. *Cell* 158(2), 288–299 (2014).

17. Ridlon JM, Kang DJ, Hylemon PB. Bile salt biotransformations by human intestinal bacteria. *J. Lipid Res.* 47(2), 241–259 (2006).
18. Nguyen TT, Ung TT, Kim NH, Do Jung Y. Role of bile acids in colon carcinogenesis. *World J. Clin. Cases.* 6(13), 577–589 (2018).
19. Cao H, Luo S, Xu M *et al.* The secondary bile acid, deoxycholate accelerates intestinal adenoma–adenocarcinoma sequence in Apc min/+ mice through enhancing Wnt signaling. *Fam. Cancer* 13(4), 563–571 (2014).
20. Roberts TG, Goulart BH, Squitieri L *et al.* Trends in the risks and benefits to patients with cancer participating in Phase I clinical trials. *JAMA* 292(17), 2130–2140 (2004).
21. Ternes D, Karta J, Tsenkova M, Wilmes P, Haan S, Letellier E. Microbiome in colorectal cancer: how to get from meta-omics to mechanism? *Trends Microbiol.* 28(5), 401–423 (2020).
22. Leystra AA, Clapper ML. Gut microbiota influences experimental outcomes in mouse models of colorectal cancer. *Genes (Basel)* 10(11), 900 (2019).
23. Kersten K, Visser KE, Miltenburg MH, Jonkers J. Genetically engineered mouse models in oncology research and cancer medicine. *EMBO Mol. Med.* 9(2), 137–153 (2017).
24. McIntyre RE, Buczacki SJA, Arends MJ, Adams DJ. Mouse models of colorectal cancer as preclinical models. *BioEssays* 37(8), 909–920 (2015).
25. Nguyen TLA, Vieira-Silva S, Liston A, Raes J. How informative is the mouse for human gut microbiota research? *Dis. Model. Mech.* 8(1), 1–16 (2015).
26. Mähler M, Bristol IJ, Leiter EH *et al.* Differential susceptibility of inbred mouse strains to dextran sulfate sodium-induced colitis. *Am. J. Physiol. Gastrointest. Liver Physiol.* 274(3), 6–9 (1998).
27. Nagalingam NA, Kao JY, Young VB. Microbial ecology of the murine gut associated with the development of dextran sodium sulfate-induced colitis. *Inflamm. Bowel Dis.* 17(4), 917–926 (2011).
28. Heijstek M, Kranenburg O, Borel Rinkes I. Mouse models of colorectal cancer and liver metastases. *Dig. Surg.* 22(1–2), 26–33 (2005).
29. Pan Q, Lou X, Zhang J *et al.* Genomic variants in mouse model induced by azoxymethane and dextran sodium sulfate improperly mimic human colorectal cancer. *Sci. Rep.* 7(1), 25 (2017).
30. Jackson SJ, Thomas GJ. Human tissue models in cancer research: looking beyond the mouse. *Dis. Model. Mech.* 10(8), 939–942 (2017).
31. Hidalgo M, Amant F, Biankin AV *et al.* Patient-derived xenograft models: an emerging platform for translational cancer research. *Cancer Discov.* 4(9), 998–1013 (2014).
32. Puig I, Chicote I, Tenbaum SP *et al.* A personalized preclinical model to evaluate the metastatic potential of patient-derived colon cancer initiating cells. *Clin. Cancer Res.* 19(24), 6787–6801 (2013).
33. Zitvogel L, Pitt JM, Daillère R, Smyth MJ, Kroemer G. Mouse models in oncoimmunology. *Nat. Publ. Gr.* 16(12), 759–773 (2016).
34. Huch M, Koo BK. Modeling mouse and human development using organoid cultures. *Dev.* 142(18), 3113–3125 (2015).
35. Kaufman MH, Evans MJ. Establishment in culture of pluripotent cells from mouse embryos. *Nature* 292, 154–156 (1981).
36. Sato T, Vries RG, Snippert HJ *et al.* Single Lgr5 stem cells build crypt-villus structures *in vitro* without a mesenchymal niche. *Nature* 459(7244), 262–265 (2009).
37. Sato T, Stange DE, Ferrante M *et al.* Long-term expansion of epithelial organoids from human colon, adenoma, adenocarcinoma, and Barrett's epithelium. *Gastroenterology* 141(5), 1762–1772 (2011).
38. Barrila J, Crabbé A, Yang J *et al.* Modeling host-pathogen interactions in the context of the microenvironment: three-dimensional cell culture comes of age. *Infect. Immun.* 86(11), 1–28 (2018).
39. Hubert CG, Rivera M, Spangler LC *et al.* A three-dimensional organoid culture system derived from human glioblastomas recapitulates the hypoxic gradients and cancer stem cell heterogeneity of tumors found *in vivo*. *Cancer Res.* 76(8), 2465–2477 (2016).
40. Xu H, Lyu X, Yi M, Zhao W, Song Y, Wu K. Organoid technology and applications in cancer research. *J. Hematol. Oncol.* 11(1), 1–15 (2018).
41. Weeber F, Ooft SN, Dijkstra KK, Voest EE. Tumor organoids as a pre-clinical cancer model for drug discovery. *Cell Chem. Biol.* 24(9), 1092–1100 (2017).
42. Roerink SF, Sasaki N, Lee-Six H *et al.* Intra-tumour diversification in colorectal cancer at the single-cell level. *Nature* 556(7702), 457–462 (2018).
43. Weeber F, van de Wetering M, Hoogstraat M *et al.* Preserved genetic diversity in organoids cultured from biopsies of human colorectal cancer metastases. *Proc. Natl Acad. Sci. USA* 112(43), 13308–13311 (2015).
44. Fujii M, Clevers H, Sato T. Modeling human digestive diseases with CRISPR-Cas9–modified organoids. *Gastroenterology* 156(3), 562–576 (2019).
45. Driehuis E, Clevers H. CRISPR/Cas 9 genome editing and its applications in organoids. *Am. J. Physiol. Gastrointest. Liver Physiol.* 312(3), G257–G265 (2017).
46. Bartfeld S. Modeling infectious diseases and host-microbe interactions in gastrointestinal organoids. *Dev. Biol.* 420(2), 262–270 (2016).

47. Sun J. Intestinal organoid as an *in vitro* model in studying host-microbial interactions. *Front. Biol. (Beijing)* 12(2), 94–102 (2017).
48. Blutt SE, Crawford SE, Ramani S, Zou WY, Estes MK. Engineered human gastrointestinal cultures to study the microbiome and infectious diseases. *Cell. Mol. Gastroenterol. Hepatol.* 5(3), 241–251 (2018).
49. Dutta D, Heo I, Clevers H. Disease modeling in stem cell-derived 3D organoid systems. *Trends Mol. Med.* 23(5), 393–410 (2017).
50. Ettayebi K, Crawford SE, Murakami K *et al.* Replication of human noroviruses in stem cell-derived human enteroids. *Science* 353(6306), 1387–1393 (2016).
51. Leslie JL, Huang S, Opp JS *et al.* Persistence and toxin production by *Clostridium difficile* within human intestinal organoids result in disruption of epithelial paracellular barrier function. *Infect. Immun.* 83(1), 138–145 (2015).
52. Aoki-Yoshida A, Saito S, Fukiya S *et al.* *Lactobacillus rhamnosus* GG increases Toll-like receptor 3 gene expression in murine small intestine *ex vivo* and *in vivo*. *Benef. Microbes* 7(3), 421–429 (2016).
53. Engevik MA, Aihara E, Montrose MH, Shull GE, Hassett DJ, Worrell RT. Loss of NHE3 alters gut microbiota composition and influences *Bacteroides thetaiotaomicron* growth. *Am. J. Gastrointest. Liver Physiol.* 305(10), G697–G711 (2013).
54. Pleguezuelos-Manzano C, Puschhof J, Rosendahl Huber A *et al.* Mutational signature in colorectal cancer caused by genotoxic *pks*⁺*E. coli*. *Nature* 580(7802), 269–273 (2020).
55. Karve SS, Pradhan S, Ward DV, Weiss AA. Intestinal organoids model human responses to infection by commensal and Shiga toxin producing *Escherichia coli*. *PLoS ONE* 12(6), 1–20 (2017).
56. Lukovac S, Belzer C, Pellis L *et al.* Differential modulation by *Akkermansia muciniphila* and *Faecalibacterium prausnitzii* of host peripheral lipid metabolism and histone acetylation in mouse gut organoids. *MBio* 5(14), 1–10 (2014).
57. Hou Q, Ye L, Liu H *et al.* *Lactobacillus* accelerates ISCs regeneration to protect the integrity of intestinal mucosa through activation of STAT3 signaling pathway induced by LPLs secretion of IL-22. *Cell Death Differ.* 25(9), 1657–1670 (2018).
58. Schilderink R, Verseijden C, Seppen J *et al.* The SCFA butyrate stimulates the epithelial production of retinoic acid via inhibition of epithelial HDAC. *Am. J. Physiol. Gastrointest. Liver Physiol.* 310(11), G1138–G1146 (2016).
59. Park J, Kotani T, Konno T *et al.* Promotion of intestinal epithelial cell turnover by commensal bacteria: role of short-chain fatty acids. *PLoS ONE* 11(5), 1–22 (2016).
60. Kaiko GE, Ryu SH, Koues OI *et al.* The colonic crypt protects stem cells from microbiota-derived metabolites. *Cell* 165(7), 1708–1720 (2016).
61. Toden S, Ravindranathan P, Gu J, Cardenas J, Yuchang M, Goel A. Oligomeric proanthocyanidins (OPCs) target cancer stem-like cells and suppress tumor organoid formation in colorectal cancer. *Sci. Rep.* 8(1), 3335 (2018).
62. Egeblad M, Nakasone ES, Werb Z. Tumors as organs: complex tissues that interface with the entire organism. *Dev. Cell.* 18(6), 884–901 (2010).
63. Okumura R, Takeda K. Roles of intestinal epithelial cells in the maintenance of gut homeostasis. *Exp. Mol. Med.* 49(5), e338 (2017).
64. Rogoz A, Reis BS, Karssemeijer RA, Mucida D. A 3-D enteroid-based model to study T-cell and epithelial cell interaction. *J. Immunol. Methods* 421, 89–95 (2015).
65. Nozaki K, Mochizuki W, Matsumoto Y *et al.* Co-culture with intestinal epithelial organoids allows efficient expansion and motility analysis of intraepithelial lymphocytes. *J. Gastroenterol.* 51(3), 206–213 (2016).
66. Noel G, Baetz NW, Staab JF *et al.* A primary human macrophage-enteroid co-culture model to investigate mucosal gut physiology and host-pathogen interactions. *Sci. Rep.* 7, 46790 (2017).
67. Wlodarska M, Luo C, Kolde R *et al.* Indoleacrylic acid produced by commensal *Peptostreptococcus* species suppresses inflammation. *Cell Host Microbe* 22(1), 25–37.e6 (2017).
68. Greten FR, Grivennikov SI. Inflammation and cancer: triggers, mechanisms, and consequences. *Immunity* 51(1), 27–41 (2019).
69. Lahar N, Lei NY, Wang J *et al.* Intestinal subepithelial myofibroblasts support *in vitro* and *in vivo* growth of human small intestinal epithelium. *PLoS ONE* 6(11), e26898 (2011).
70. Lei NY, Jabaji Z, Wang J *et al.* Intestinal subepithelial myofibroblasts support the growth of intestinal epithelial stem cells. *PLoS ONE* 9(1), e84651 (2014).
71. Pastula A, Middelhoff M, Brandtner A *et al.* Three-dimensional gastrointestinal organoid culture in combination with nerves or fibroblasts: a method to characterize the gastrointestinal stem cell niche. *Stem Cells Int.* 2016, 3710836 (2016).
72. Ihara S, Hayakawa Y, Konishi M, Hirata Y, Koike K. 3D co-culture system of intestinal organoids and dendritic cells to study epithelial differentiation. *Gastroenterology* 152(5), S134–S135 (2017).
73. Westphalen CB, Asfaha S, Hayakawa Y *et al.* Long-lived intestinal tuft cells serve as colon cancer-initiating cells. *J. Clin. Invest.* 124(3), 1283–1295 (2014).
74. Takahashi Y, Sato S, Kurashima Y *et al.* Reciprocal inflammatory signaling between intestinal epithelial cells and adipocytes in the absence of immune cells. *EBioMedicine* 23, 34–45 (2017).

75. Kasendra M, Tovaglieri A, Sontheimer-Phelps A *et al.* Development of a primary human small intestine-on-a-chip using biopsy-derived organoids. *Sci. Rep.* 8(1), 2871 (2018).
76. Grün D, Lyubimova A, Kester L *et al.* Single-cell messenger RNA sequencing reveals rare intestinal cell types. *Nature* 525(7568), 251–255 (2015).
77. Fong W, Li Q, Yu J. Gut microbiota modulation: a novel strategy for prevention and treatment of colorectal cancer. *Oncogene* 39(26), 4925–4943 (2020).
78. Boehnke K, Iversen PW, Schumacher D *et al.* Assay establishment and validation of a high-throughput screening platform for three-dimensional patient-derived colon cancer organoid cultures. *J. Biomol. Screen.* 21(9), 931–941 (2016).
79. Kondo J, Ekawa T, Endo H *et al.* High-throughput screening in colorectal cancer tissue-originated spheroids. *Cancer Sci.* 110(1), 345–355 (2019).
80. Park SE, Georgescu A, Huh D. Organoids-on-a-chip. *Science* 364(6444), 960–965 (2019).
81. van de Wetering M, Francies HE, Francis JM *et al.* Prospective derivation of a living organoid biobank of colorectal cancer patients. *Cell* 161(4), 933–945 (2015).
82. Fujii M, Shimokawa M, Date S *et al.* A colorectal tumor organoid library demonstrates progressive loss of niche factor requirements during tumorigenesis. *Cell Stem Cell* 18(6), 827–838 (2016).
83. Vlachogiannis G, Hedayat S, Vatsiou A *et al.* Patient-derived organoids model treatment response of metastatic gastrointestinal cancers. *Science* 359(6378), 920–926 (2018).
84. Huch M, Knoblich JA, Lutolf MP, Martinez-Arias A. The hope and the hype of organoid research. *Development* 144(6), 938–941 (2017).
85. Grabinger T, Luks L, Kostadinova F *et al.* *Ex vivo* culture of intestinal crypt organoids as a model system for assessing cell death induction in intestinal epithelial cells and enteropathy. *Cell Death Dis.* 5(5), e1228 (2014).
86. Gjorevski N, Sachs N, Manfrin A *et al.* Designer matrices for intestinal stem cell and organoid culture. *Nature* 539(7630), 560–564 (2016).
87. Drost J, van Jaarsveld RH, Ponsioen B *et al.* Sequential cancer mutations in cultured human intestinal stem cells. *Nature* 521(7550), 43–47 (2015).
88. Masramon L, Vendrell E, Tarafa G *et al.* Genetic instability and divergence of clonal populations in colon cancer cells *in vitro*. *J. Cell Sci.* 119(8), 1477–1482 (2006).
89. Yu F, Hunziker W, Choudhury D. Engineering microfluidic organoid-on-a-chip platforms. *Micromachines (Basel)* 10(3), 1–12 (2019).
90. Williamson IA, Arnold JW, Samsa LA *et al.* A high-throughput organoid microinjection platform to study gastrointestinal microbiota and luminal physiology. *Cell. Mol. Gastroenterol. Hepatol.* 6(3), 301–319 (2018).
91. O'Rourke KP, Loizou E, Livshits G *et al.* Transplantation of engineered organoids enables rapid generation of metastatic mouse models of colorectal cancer. *Nat. Biotechnol.* 35(6), 577–582 (2017).
92. Roper J, Tammela T, Cetinbas NM *et al.* *In vivo* genome editing and organoid transplantation models of colorectal cancer. *Nat. Biotechnol.* 35(6), 569–576 (2017).
93. Watson CL, Mahe MM, Munera J *et al.* An *in vivo* model of human small intestine using pluripotent stem cells. *Nat. Med.* 20(11), 1310–1314 (2014).
94. Tsai YH, Nattiv R, Dedhia PH *et al.* *In vitro* patterning of pluripotent stem cell-derived intestine recapitulates *in vivo* human development. *Development* 144(6), 1045–1055 (2017).
95. Múnera JO, Sundaram N, Rankin SA *et al.* Differentiation of human pluripotent stem cells into colonic organoids via transient activation of BMP signaling. *Cell Stem Cell* 21(1), 51–64.e6 (2017).
96. Holloway EM, Capeling MM, Spence JR. Biologically inspired approaches to enhance human organoid complexity. *Development* 146(8), dev166173 (2019).



Contact the Sartorius team

North America

Sartorius Corporation
300 West Morgan Road
Ann Arbor, Michigan, 48108
USA
Phone: +1 734 769 1600
E-Mail: orders.US07@sartorius.com

APAC

Sartorius Japan K.K.
4th Floor, Daiwa Shinagawa North Bldg.
1-8-11 Kita-Shinagawa 1-chrome
Shinagawa-ku,
Tokyo 140-0001
Japan
Phone: +81 3 6478 5202
E-Mail: orders.US07@sartorius.com

Europe

Sartorius UK Ltd.
Longmead Business Centre
Blenheim Road
Epsom
Surrey, KT19 9QQ
United Kingdom
Phone: +44 1763 227400
E-Mail: euorders.UK03@sartorius.com

 **Find out more:** www.sartorius.com/incucyte

 **For questions, email:** AskAScientist@sartorius.com





Contact us

Editorial Department

Senior Editor

Tristan Free

tfree@biotechniques.com

Business Development and Support

Commercial Director

Evelina Rubio Hakansson

e.rubiohakansson@future-science-group.com

This supplement is brought to you by *BioTechniques* in association with

SARTORIUS